이학석사 학위논문

건강인 말초혈액으로부터 항원 특이적 T 세포 분석 및 개발

Analysis and development of antigen-specific T cells from healthy donor PBMC

울 산 대 학 교 대 학 원

의 과 학 과

김 지 형

건강인 말초혈액으로부터 항원 특이적 T 세포 분석 및 개발

지 도 교 수 이 희 진

이 논문을 이학 석사학위 논문으로 제출함

2024 년 2 월

울 산 대 학 교 대 학 원

의 과 학 과

김 지 형

김지형의 이학 석사학위 논문을 인준함

심사위원 공 경 엽 (인)

심사위원 이 희 진 (인)

심사위원 유 태 경 (인)

울 산 대 학 교 대 학 원

2024 년 2 월

Abstract

Adoptive cell therapy using antigen-specific T cells is a promising treatment modality for cancer patients. Therefore, novel methods for isolating antigen-specific T cells and identifying corresponding T cell receptors are needed to find effective targets for adoptive cell therapy. We evaluated the proliferation of antigen-specific T cells in PBMC by staining them with CFSE dye and stimulating them with antigen peptides to isolate antigen-specific T cells. In addition, we analyzed CMV and EBV-specific TCR sequences and transduction of specific TCRs to T cells and validation of TCR-T. Isolated CD8+ cells from healthy donor PBMC exhibited the most proliferation in response to CMV and EBV at day 7, under G2 conditions using minimal IL-2. TCR sequence analysis also demonstrated responsiveness to CMV and EBV peptides in vitro. Reactivity was confirmed in all 10 types of CMV-specific TCR candidates and in EBV TCR 3. In conclusion, this methodology can be a cost-effective and time-efficient way to identify neoantigen-specific T cells and TCRs, which may serve as novel potential targets for immunotherapy.

CONTENTS

Lists of figures and table

Introduction

In recent times, several immunotherapeutic strategies harnessing the immune system's specificity to target and eliminate tumors have garnered significant attention. Despite the success of immune checkpoint inhibitor (ICI) therapies such as anti-CTLA-4 or anti-PD-1/PD-L1 inhibitors, only 15-30% of solid tumor patients benefit from ICIs.(1) Immune checkpoint inhibitors (ICIs) function by relieving immune suppression caused by immune checkpoint molecules on cytotoxic T cells, thereby promoting immune activation.(2, 3) However, lack of anticancer T cells in the tumor microenvironment (TME) is one of resistant mechanisms toward ICIs.(4, 5) Anticancer T cells can be cultured and used as adoptive cell therapy (ACT). ACT include transfer of cultured natural T cells derived from peripheral blood mononuclear cells (PBMCs) and tumor-infiltrating lymphocytes (TILs) and engineered T cells including chimeric antigen receptor T cell (CAR-T) and T cell receptor engineered T cell (TCR-T). CAR-T consists of three domains: single-chain variable fragment (scFv), immunoreceptor tyrosine-based activation motif (ITAM), and CD3, which can recognize antigens and activate T cells. However, CAR-T is limited to recognizing only cell surface membrane proteins, which constitute approximately 1% of the total proteins expressed in cells.(6) CAR-T has shown clinical success in hematological malignancies and several products have been approved and applied in daily practice, whereas it has shown limited clinical success in solid tumors.(7) TCR-T has a TCR that recognizes specific major histocompatibility complex (MHC)-peptide antigen complex. A TCR consists of an alpha chain and a beta chain. Targets for TCR-T are antigens derived from intracellular and surface proteins, which is a strength of TCR-T over CAR-T since most of antigens are present intracellularly.(6)

Antigens are recognized by the amino acid sequence of complementarity-determining region 3 (CDR3) in the alpha and beta chains. CDR3 is determined through specific recombination of variable (V), diversity (D), and joining (J) gene segments, and reacts with various antigens through numerous recombination.(8, 9) It is important to analyze CDR3, which is a site that specifically binds antigen. DNA sequencing technologies include 454/Roche platform based on pyrosequencing technology, Illumina/Solexa platform, and Ion Torrent/Life Technologies based on Sanger-sequencing technology.(10-12) The advancement of next-generation sequencing (NGS) technology has enabled the analysis of TCR sequences. In addition, the development of single-cell analysis made it possible to analyze alpha and beta pairs of TCR sequences.(11, 13) With the development of single-cell analysis technology, immune repertoire research is becoming more and more important because it is possible to increase the level of repertoire analysis by accurately identifying and analyzing pairs rather than analysis of a group of cells.(13)

Tumor antigens consist of tumor-associated antigens (TAAs) and tumor-specific antigens (neoantigens). NY-ESO-1 and Epstein Barr Virus (EBV) are well known TAAs.(14, 15) It is important to identify and selectively classify specific T cells recognizing tumor antigens.(13) There are several methods for identifying antigen-specific T cells including sorting of T cells using MHC-tetramer or based on expression of markers such as 4-1BB and PD-1.(16-19)

In this paper, we suggested 3 steps for the development of TCR-T; 1) isolation of antigen-specific T cells, 2) analyzing antigen-specific TCR sequences, 3) transduction of specific TCRs to T cells and validation of TCR-T. We used well-known antigens: EBV and cytomegalovirus (CMV).

Materials and methods

Human samples

PBMCs were isolated from whole blood acquired from healthy donors. Informed consent was obtained from the donors (IRB#2017-0784). Separation of blood cells was performed using density centrifugation (Ficoll Paque, Cytiva). After isolation, PBMCs were washed two times using phosphate buffered saline (PBS, Biowest, Nuaillé, France) containing 2% fetal bovine serum (FBS, Corning, Arizona, USA). Washed healthy donor PBMCs were immediately used or stored in a deep-freezer (-80℃).

HLA typing

HLA typing from PBCM from healthy donor was performed by requesting Biowithus (Seoul, South Korea), a company specializing in the development and manufacture of in vitro diagnostic reagents.

ELISpot assay

Human IFN-γ ELISPOT assays (MABTECH) were conducted according to the manufacturer's instructions. PBMCs (1e5 cells/well) isolated from healthy donors were cultured in CTL medium supplemented with 10% FBS and 1% penicillin streptomycin for 24 h at 37°C, 5% CO_2. CMV and EBV peptides (Synpeptide) were dissolved in DMSO and added to the culture system at a concentration of 1 ug/ml as a stimulating antigen. The spots were quantified using an ELISPOT reader (iSpotSpectrum, AID, Strassberg, Germany) and the results were reported as the number of spot-forming units (SFU) per well.

Staining of PBMC with CFSE dye and stimulation with antigen peptide

The isolated PBMCs were suspended in PBS and treated with 0.5 uM of carboxyfluorescein diacetate succinimidyl ester (CFSE, Thermofisher scientific, Massachusetts, USA). And after incubation at RT for 20 minutes, the stabilization process was performed through adding 5 times 3% CTL media of the amount of staining. Stained PBMCs were seeded into 96-well plate (1 e5 cells/well) or 15 ml polypropylene (PP) tube (1 e6 cells/tube). PBMCs were stimulated with CMV peptide (NLVPMVATV**,** 1 ug/ml) or EBV peptides (EBV-1 LTAGFLIFL, EBV-2 CLGGLLTMV, EBV-3 FLYALALLI, EBV-4 TYGPVFMCL, EBV-5 RYCCYYCLTL**,** and EBV-6 FLYALALLL, 1 μg/ml). Stimulated cells were cultured without or with IL-2 (100 IU/ml) and cultured for 7 days and 9 days in a humidified atmosphere of 5% CO_2 at 37°C to determine T cell proliferation.

Flow cytometry analysis

Cultured PBMCs in 96-well plates were harvested after 7 days or 9 days and washed with FACS buffer (2% FBS contained DPBS). The pellet was re-suspended in 1 ml FACS buffer and stained with Human Tru-Stain FcX (Fc Receptor Blocking Solution, Biolegend, San Diego, USA) at room temperature. After 5 min PBMCs were stained with APC/Cyanine7 anti-human CD3 antibody, PerCP/Cyanine5.5 anti-human CD8 antibody (Biolegend), and cells were packed aluminum foil. And then cells were incubated at room temperature. After 20 min, PBMCs were washed 1 ml FACS buffer, centrifuge, and suspended in 200 μl DAPI mixed FACS buffer. FACS Canto II-based flow cytometry was conducted to measure the samples. The analysis of the $CD8^+$ T cells is based on five lymphocyte gates (1) FSC versus SSC, (2) FSC-A versus FSC-H (singlets gate), (3) FSC-

A versus Pacific Blue-A (Live cells gate), (4) FSC-A versus APC/Cy7 CD3 ($CD3^+$ cells gate), and (5) FSC-A versus PerCP/Cy5.5 CD8 ($CD8^+$ cells gate). Now the decrease of CFSE dye intensity in expanded $CD8^+$ T cells for identification $CD8^+$ T cell proliferation platform was measured. Data analysis was performed using FlowJo.7.6.5 software. Flow Jo offers a visual representation along with details for each generation within the subset. Additionally, the proliferation platform furnishes data regarding the portion of cells from the population that underwent proliferation, specifically for CMV or EBV-specific T cells.

Sorting analysis

CFSE stained PBMCs in PP tubes were harvested after 7 days or 9 days and washed with FACS buffer. The PBMCs were stained with Human Tru-Stain FcX (Fc Receptor Blocking Solution, Biolegend) at room temperature. After 5 min PBMCs were stained with APC/Cyanine7 anti-human CD3 antibody, PerCP/Cyanine5.5 anti-human CD8 antibody (Biolegend), APC anti-human CD137 (4-1BB), PE anti-human CD279 (PD-1), and cells were packed aluminum foil. And then cells were incubated at room temperature. After 20 min, PBMCs were washed 1 ml Sorting buffer (1% FBS contained DPBS), centrifuge, and suspended in 200 µl DAPI mixed Sorting buffer. FACS (The BD FACSCanto™ II Flow Cytometer, New jersey, USA) was conducted to measure the samples. The analysis of the $CD8^+$ T cells and is based on five lymphocyte gates (1) FSC versus SSC, (2) FSC-A versus FSC-H (singlets gate), (3) FSC-A versus Pacific Blue-A (Live cells gate), (4) FSC-A versus APC/Cy7 CD3 ($CD3^+$ cells gate) and (5) FSC-A versus PerCP/Cy5.5 CD8 ($CD8^+$ cells gate). Now the decrease of CFSE dye intensity in expanded $CD8^+$ T cells for identification $CD8^+$ T cell proliferation platform was measured.

Gated CFSE decreased $CD8^+$ and $CD8^-$ T cells are sorted and collected in CTL medium. Data analysis was performed using FlowJo.7.6.5 software. Flow Jo displays a visual representation and provides details about each generation within the subset. Furthermore, the proliferation platform supplies information about the proportion of cells from the original population that have undergone proliferation, specifically focusing on CMV or EBV-specific T cells.

Single-cell VDJ library construction and sequencing

Sorted T cells were centrifuged (1,500 rpm / 5 min / RT) to remove the supernatant, and then used for preparation of VDJ library. Single-cell libraries were prepared from CMV or EBV-specific T cells according to manufacturer's protocol of Chromium Next GEM Single Cell 5' v2 Reagent Kits (10× Genomics, California, USA). The sorted cells and kit reagents were combined with gel beads that contained barcoded oligonucleotides (UMIs) and oligo dTs, which are utilized for the reverse transcription of polyadenylated RNAs. This resulted in the formation of a singular gel bead-in-emulsion (GEM). The barcoded cDNAs within each GEM were consolidated for PCR amplification, and adapter sequences along with sample indices were introduced. Single-cell libraries of gene expression and VDJ were sequenced on the Illumina Novaseq 6000 sequencing platform with paired-end 100 bp and 150 bp reads, respectively.

Analysis of sequence data

Sequencing data generated by single-cell platforms, was analyzed using the 10X

Genomics platform such as Cellranger multi or Cellranger vdj. Gene expression data and TCR data were aligned with GRCh38-2020-A and refdata-cellranger-vdj-GRCh38-alts-ensembl-5.0.0, respectively. Filtered gene expression data matrix as an initial Cellranger outputs was imported using the Read10X function of Seurat R package. nCount_RNA (number of UMIs), nFeature_RNA (number of detected genes (features)), percent_mito (frequency of reads that map to mitochondrial genes), and percent_ribo (frequency of reads that map to ribosomal genes) were quantified in each sample were calculated using summary and PercentageFeatureSet functions. Using subset function, the subgroups were manually classified for 4 T cell subsets: 1) $CD3E^{+}CD4^{+}CD8^{+}$, 2) $CD3E^{+}CD4^{+}CD8^{-}$, 3) $CD3E^{+}CD4^{-}CD8^{+}$, 4) $CD3E^{+}CD4^{-}CD8^{-}$ and counted for the number of cells in each group. The scRepertoire R package was used for the TCR clonotype analysis. The contig list per each cell barcode was generated using combineTCR function. A unique clonotype was defined as both same V(D)J and CDR3 nucleotide sequences of TCR alpha/beta chains. Total count or relative frequency of unique clonotypes were quantified in each sample. In case of EBV-specific T cell, clonotypic information of a T cell subset was preferentially attached it to our Seurat object using the combine Expression function and the relative proportion of clonotypes was calculated in each group.

Searching in TCR database

Antigen-specificity of top 10 dominant clones in each sample was confirmed using VDJmatch tools [https://github.com/antigenomics/vdjmatch] with a latest version VDJdb [https://vdjdb.cdr3.net/]. VDJmatch was carried out with an input data containing V, D, J

gene, CDR3 nucleotide sequences, CDR3 amino acid sequences and ran separately for TRA and TRB genes (e.g., -R TRB). Matching against the Immune epitope database (IEDB) [http://www.iedb.org/] was performed using TCRMatch tools [https://github.com/IEDB/TCRMatch] as an input data for only CDR3beta amino acid sequences.

Generation of antigen-specific TCR-T construct

The CMV or EBV-specific TCR analyzed to produce CMV or EBV-specific TCR was obtained plasmid by requesting gene synthesis from the BIONICS company. For CMV-specific TCR construction, first, both FUGW-1G4-IRES-GFP plasmid and pUC-IRES plasmid were digested using XbaI (NEB, Massachusetts, USA) and BstXI (NEB) enzymes. Digested genes were electrophoresis at 100V in 1% agarose gel. The bands corresponding to 8,921 bp and 601 bp, respectively, were identified and DNA was obtained using a gel extraction kit (QIAGEN, Hilden, Germany). Each DNA fragment obtained a FUGW-IRES-GFP plasmid through a ligation process using T4 ligase (Thermo scientific). CMV specific TCR plasmids synthesized and FUGW-IRES-GFP plasmid were digested using XbaI and BstXI or BsiWI (NEB) and BstXI enzymes. The digested genes identified through 1% agarose gel electrophoresis obtained DNA using a gel extraction kit, and 10 FUGW-CMV specific TCR-IRES-GFP plasmids were cloned through T4 ligase. Digestion process was all reacted at 37℃ for 1 hour, and the ligation process was reacted at 22℃ for 10 minutes.

For EBV-specific TCR construction, the mTCRβ constant gene was amplified from the FUGW-1G4-IRES-GFP plasmid through PCR to obtain a gene fragment. Then, the

FUGW-1G4-IRES-GFP plasmid and the amplified mTCRβ constant gene were digested using XbaI and BstBI enzymes. Digested DNA fragments were obtained by gel extraction of 9,517 bp and 456 bp bands, respectively, through 1% agarose gel electrophoresis. The DNA fragment was ligated using T4 ligase and cloned into the FUGW-mTCRβ constant-IRES-GFP plasmid. The FUGW-mTCRβ constant-IRES-GFP plasmid and the synthesized EBV-specific TCR plasmid were digested using XbaI and BlpI (NEB) or BsiWI and BlpI enzymes. DNA of the degraded genes identified through 1% agarose gel electrophoresis was obtained using a gel extraction kit, and five FUGW-EBV-specific TCR-IRES-GFP plasmids were cloned through T4 ligase. Digestion process was reacted at 37℃ for 1 hour or 4 hours, and the ligation process was reacted at 22℃ for 10 minutes.

Production lentiviral vectors

Lenti-X 293T cells (4e6) were seeded in a 175T flask and replaced with antibiotics-free media after 3 days. Lipofectamine, lentiviral packaging plasmids (pMDL-prre, pRSV-rev and pMD2.G) and the selected TCR plasmid were placed in the culture media of Lenti-X 293T cells and incubated for 2 days. The supernatant of Lenti-X 293T cell was obtained, centrifuged (2000 rpm/10 min/RT), and passed through 0.45 filter. The passed supernatant was mixed with a concentrator (TAKARA, Shiga, Japan) in a ratio of 3:1, and incubated at 4˚C for 2 days. After that, the mixture was centrifuged (4,000 rpm/2 h/4℃), and the prepared sample was stored at -80℃ for use. To confirm the titer of the prepared lentiviral particles, we measured the titer of p24 using an ELISA method with a plate coated with anti-HIV p24 capture antibody according to the manufacturer's (TAKARA) instructions.

Cell transduction

For Jurkat (TCR KO)-NFAT-Luc cell line transduction, 1e6 cells were seeded in a 24 well plate, treated with TCR lentiviral particles and protamine, and centrifuge (800 g/90 min/32°C) was done. Transducing cells were incubated in a CO_2 incubator at 37°C for 1 hour, and then cultured in a 25T flask at 5e5 cells/ml. In addition, the TCR expression in transduced Jurkat-NFAT-Luc TCR KO cells was confirmed at Day 3 and Day 7 through flow cytometry analysis.

For PBMC transduction, PBMCs were stimulated with TransAct (100 ul/2e7 cells, Miltenyi Biotec, Bergisch Gladbach, Germany) and IL-2 (20 IU/ml, Boehringer Ingelheim RCV GmbH & Co.KG) for 2 days. Activated PBMCs were collected and 2e6 cells were seeded in a 24 well plate. Cells were treated with TCR lentiviral particles and protamine, and centrifuge (800 g/90 min/32°C) was done. Transduced cells were incubated in a CO_2 incubator at 37°C for 1 hour, and then cultured in a 25T flask at 5e5 cells/ml. In addition, the TCR expression in transduced primary T cells was confirmed at 1 and 2 weeks through flow cytometry analysis.

Co-culture of T cells and target cells and luciferase or IFN-γ ELISA assay

T2 cells or T2-Luc cells was pulsed with the antigen peptide corresponding to each TCR (100 ug/ml) and β2m (3 ug/ml, BD, New Jersey, USA), and incubated at room temperature for 2 hours. For T cell activation assay, Jurkat (TCR KO)-NFAT-Luc cells with or without transduction and T2 cells with or without antigen peptide pulsing were seeded at 10:1 in a white 96 well plate and incubated in a 37℃ CO_2 incubator for 24 hours. For IFN- γ ELISA assay, primary T cells with or without transduction and T2 cells with or without antigen peptide pulsing were seeded at 4:1 in a 96 well plate and incubated in a 37℃ CO_2 incubator for 24 hours. For cytotoxicity assay, primary T cells with or without transduction and T2-Luc cells with or without antigen peptide pulsing were seeded at 30:1, 10:1, 3:1, and 1:1 in a white 96 well plate and incubated in a 37℃ CO_2 incubator for 24 hours. The reactivity of co-cultured T cells and target cells was confirmed through luciferase assay and IFN-γ ELISA assay. For the luciferase assay, 24 hours after co-culture, the white 96-well plate was centrifuged (1,500 rpm/5 min/RT) to spin down the cells and 100 μl of supernatant was removed. Afterwards, 100 μl of luciferin (Promega) prepared according to the manufacturer's instructions was added and mixed, and luminescence was measured using a microplate reader (Glomax, Promega, Wiscon-sin, USA). For the IFN-γ ELISA assay, the co-cultured plate was centrifuged (1,500 rpm/5 min/RT) to remove all cells, and then 100 μl of the supernatant was used for the IFN-γ ELISA analysis. For the ELISA analysis, the concentration of INF-γ was measured using a plate coated with anti-human IFN-γ antibody and a human IFN-γ ELISA kit (Coma Biotech, Seoul, Korea)

Results

1) Isolation of antigen-specific T cells

1-1) Screening of T cell pools to identify appropriate donors

To identify CMV or EBV-specific T cells restricted to HLA-A*02:01, we screened PBMCs derived from healthy donors with an HLA-A*02:01 allele using ELISpot assay after stimulation with CMV and EBV peptides. Among the six healthy donor PBMCs, PBMCs with high reactivity with CMV peptide were PBMC21002, PBMC21003, and PBMC21010. In addition, the results of EBV peptide reactivity showed reactivity in all PBMCs except PBMC21003 in EBV-1, and EBV-2 showed higher reactivity in PBMC21002 compared to other PBMCs. EBV-3 showed higher reactivity in PBMC21002 and PBMC21010, and EBV-4 and 5 showed higher reactivity in PBMC21002. Overall, it was determined that PBMC21002 and PBMC21010 were reactive with EBV peptides (Fig. 1).

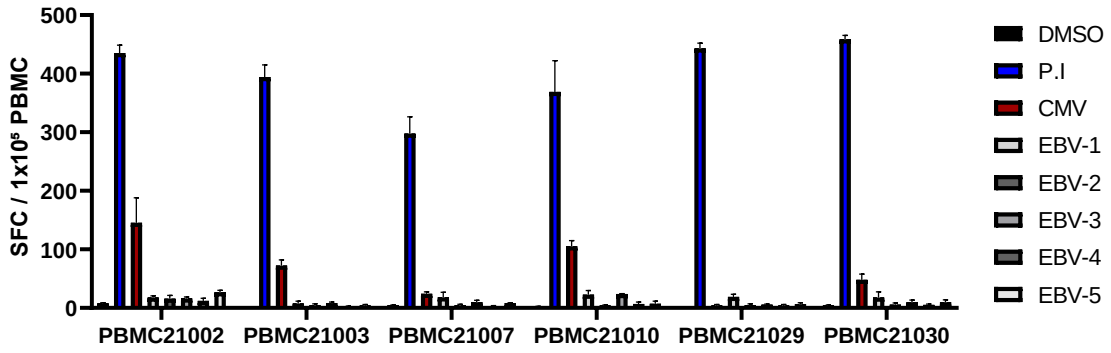

Fig. 1. Investigation of responses to CMV and EBV peptides in healthy PBMCs. To confirm the reactivity with CMV and EBV peptides in healthy donor PBMCs having the phenotype of HLA-A*02:01, each PBMCs was treated with the peptides and ELISpot assay was performed 24 hours later.

1-2) Optimizing methods for distinguishing activated T lymphocytes

When the CFSE dye is stained on the cells, the fluorescence value is decreased as the cell proliferation occurs, so it is a dye that can measure the proliferation level of the cells. Since proliferation occurs when T cells are activated with corresponding antigens, we planned to isolate the activated PBMCs by using the CFSE dye to identify antigen-specific T cells. Using CMV peptide and PBMC21002 with proven reactivity, four culture conditions (G1-G4) based on different IL2 supplementation schedules were compared to find the optimal condition in which proliferation of T cells occurs most (Table 1). The experiment was conducted for 9 days under all four conditions, and the media change was performed three times on Day 2, Day 4, and Day 7. The experiment was performed on a 96-well plate, and FACS analysis was conducted on Day 7 and Day 9. Proliferation of $CD3^+$ T cells was higher on Day 9 than on Day 7, but DMSO group also showed proliferation of T cells in all four conditions on Day 9. Therefore, it was considered to be better to analyze on Day 7 than on Day 9. Proliferation on Day 7 confirmed that G2, G3, and G4 responses were better than G1 (Fig. 2A).

Since more cells are needed than cells used in a 96-well plate to perform single cell TCR-seq of activated and proliferated cells, the scale was increased, and the same culture conditions were tested in 15 ml PP tubes. The results in the PP tube were similar to the results of the experiments performed on a 96-well plate. It was confirmed that the proliferation of G2, G3 and G4 was better than that of G1 (Fig. 2B).

The experiment using the PP tube was performed using another healthy donor PBMC21010 (Fig. 2C). Proliferation in the G1 condition was not seen at all differently from that of PBMC21002, but proliferation of T cells by CMV peptide was similar to

PBMC21002 in the G2 or G3 condition. The G4 condition resulted in less proliferation than the G2 or G3 condition. No proliferation occurred in Day 7, but proliferation of T cells was observed in Day 9 for negative control group (DMSO). Therefore, we established the conditions by isolating T cells on Day 7 under the conditions of G2 using minimal IL-2.

Table 1. Four conditions to find an optimal condition for antigen activation

Date	**Day 0**	**Day 1**	**Day 2**	**Day 3**	**Day 4**	**Day 5**	**Day 6**	**Day 7**	**Day 8**	**Day 9**
Media change	-	-	O	-	O	-	-	O (FACS)	-	(FACS)
G1	-		-		-			-		
G2	-		IL-2		-			-		
G3	-		IL-2		-			IL-2		
G4	-		IL-2		IL-2			IL-2		

A.

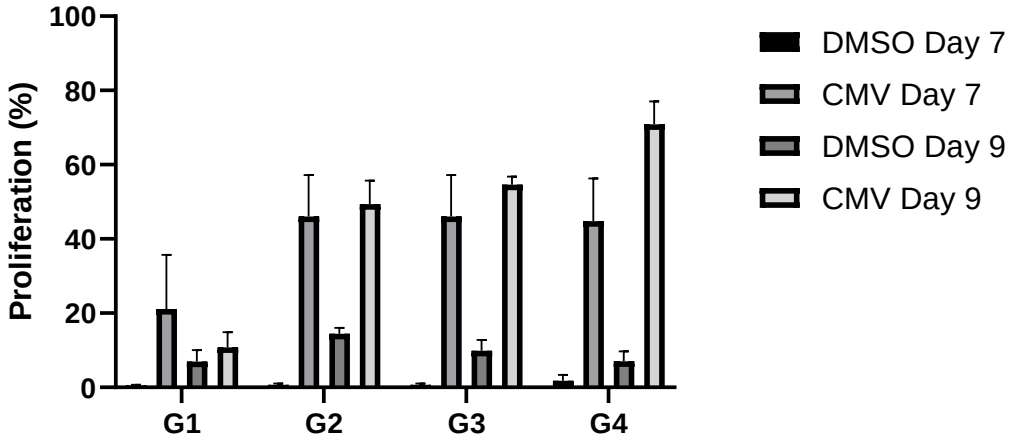
Proliferation (%)
100
80
60
40
20
0
G1
G2
G3
G4
DMSO Day 7
CMV Day 7
DMSO Day 9
CMV Day 9

B.

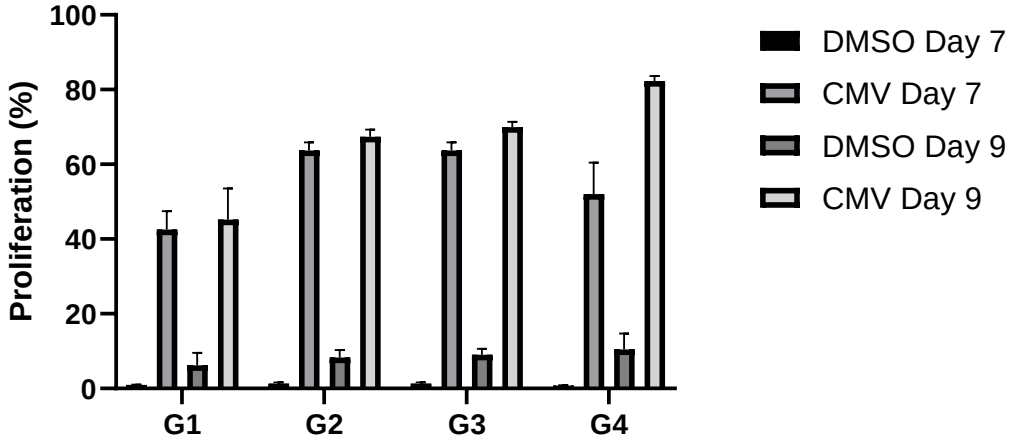
Proliferation (%)
100
80
60
40
20
0
G1
G2
G3
G4
DMSO Day 7
CMV Day 7
DMSO Day 9
CMV Day 9

C.

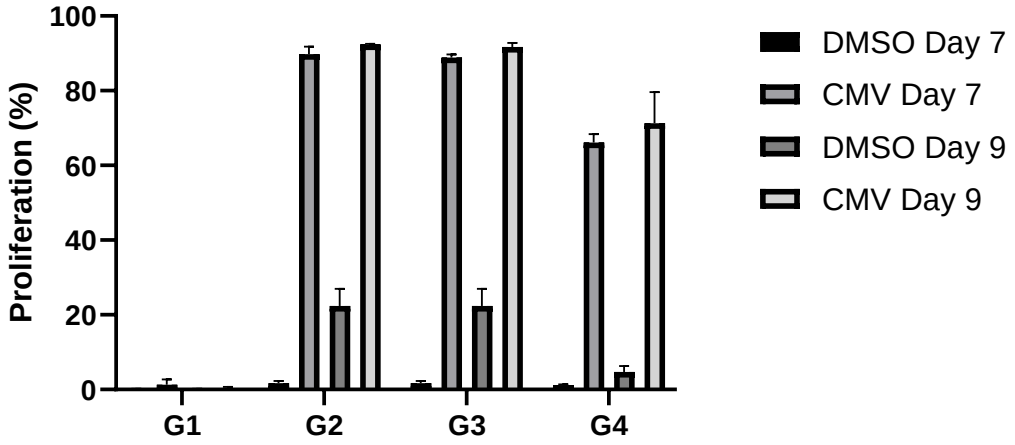

Fig. 2. Proliferation of T cells according to four different culture conditions. A. Measurement of proliferation of T cells in PBMC21002 stained with CFSE dye after activation with CMV peptide in 96 well plate. B. Measurement of proliferation of T cells in stained PBMC21002 in response to CMV peptide in PP tube. C. Measurement of proliferation of T cells in another healthy donor PBMC21010 in response to CMV peptide in PP tube.

1-3) Sorting of activated T cells

Based on the optimal condition of proliferation for sorting, the same PBMCs were used to separate T cells reacting with CMV peptide or EBV peptide mix. PBMC 21002, PBMC21003, and PBMC21010, which had reactivity to the CMV peptide, were cultured in PP tube under G2 condition. To obtain antigen specific $CD8^+$ T cells, we sorted cells based on CFSE staining and CD8 positivity. Proliferation of CMV or EBV stimulated T cells was observed at 10% and 2-3% on Day 7, respectively (Fig. 3A, B). The number of

sorted cells in response to CMV and EBV was 3.4e4 and 2.6e5 for PBMC21002, respectively, 2.9e4 and 4e3 for PBMC21003, respectively, and 9.5e5 and 1.6e6 for PBMC21010, respectively (Table 2). All these isolated cells were used for TCR sequencing.

A.

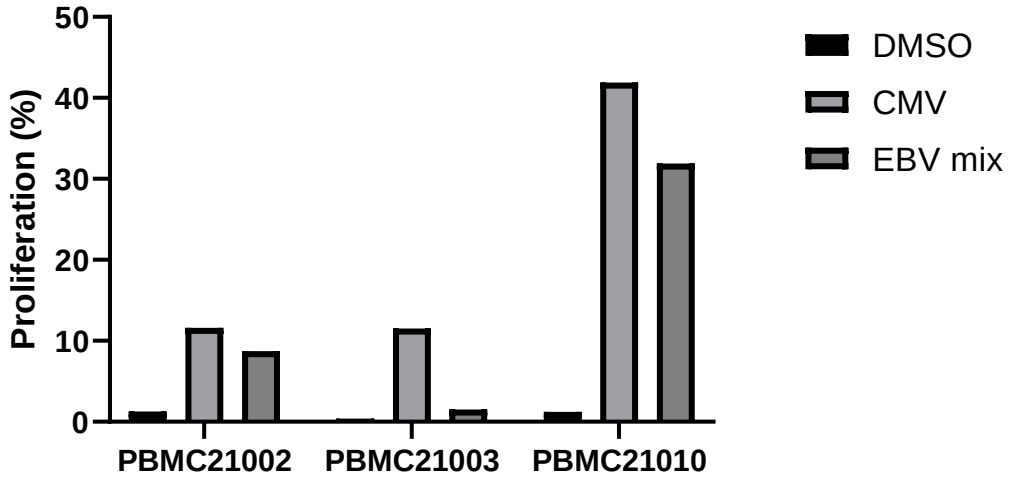

B.

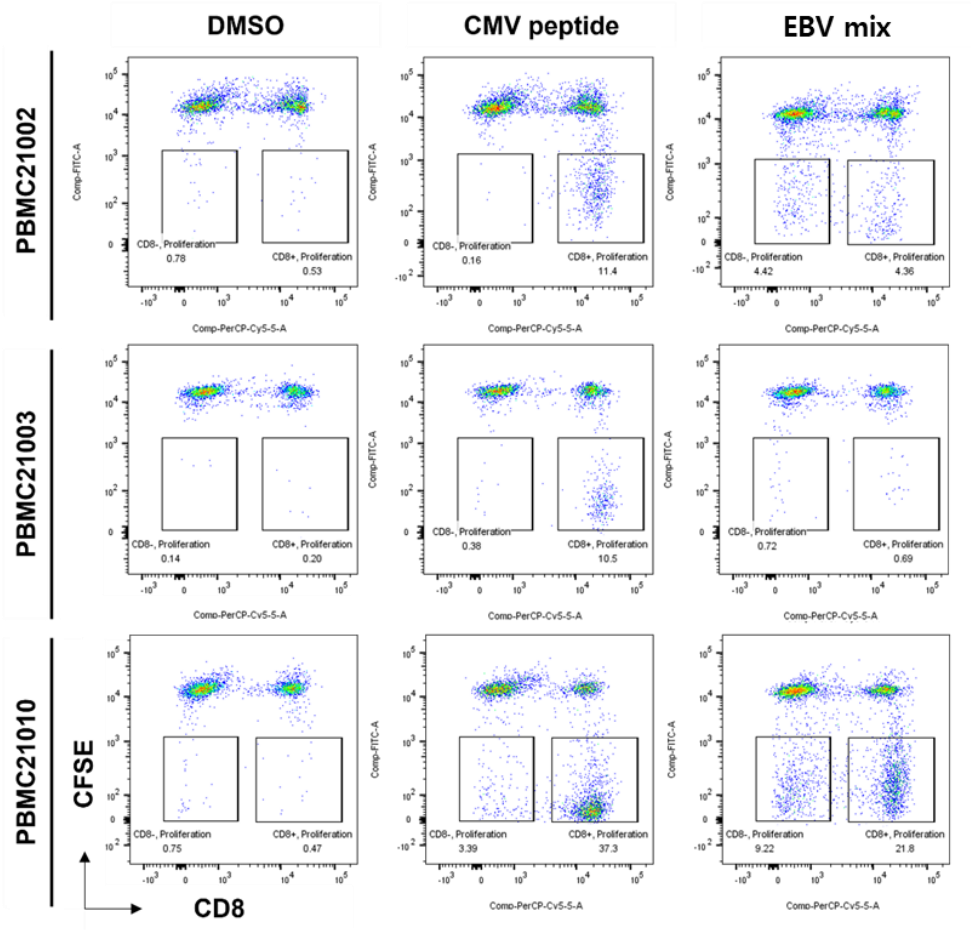

Fig. 3. Sorting of activated cells from healthy donor PBMC21002, PBMC21003, and 21010 on Day 7. A. Proliferating cells after activation with CMV peptide or EBV peptide mix are assessed by CFSE staining analysis and sorted from PBMC 21002,21003, and 21010. B. Flow cytometry analysis in $CD3^+$ T cells through the CFSE staining.

Table 2. Number of sorted CFSE negative cells reacted with CMV peptide or EBV peptides mix

PBMC	GROUP	$CD8^-/CFSE^-$	$CD8^+/CFSE^-$
PBMC 21002	CMV	491	34,120
	EBV	126,061	129,037
PBMC 21003	CMV	1,195	27,894
	EBV	1,974	2,810
PBMC 21010	CMV	76,200	875,918
	EBV	463,562	1,130,494

2) Analysis of antigen-specific TCR sequences

2-1) CMV-specific TCR sequences

Based on single cell gene expression profile, there was the frequency of 81.4% (2,297/2,822), 92.6% (1,160/1,253), and 91.0% (3,846/4,225) of $CD3^+$ T cells per total cells and of which 92% (2,113/2,297), 97.5% (1,131/1,160), and 97.2% (3,739/3,846) were $CD3E^+CD4^-CD8^+$ cells in PBMC21002, 21003, and 21010, respectively (Table 3). $CD8^+$ T cells were analyzed using the output of the CellRanger vdj.

Dominant clones were expressed at high levels and top 10 clonotypes were also present in > 80 % in all healthy donors (Table 4). Antigen-specificity of top 10 clonotypes in each sample was analyzed using searching tools (i.e. VDJtools and VDJMatch) in the database (VDJDB and IEDB) with information of known TCRs (Table 5).

TCRα or TCRβ were compared to the information of TCR database that includes TCR specific for the various antigens. Several clonotypes (top 2 and top 6 in PBMC21002, top 4 and top 5 in PBMC21003, and top 2 in PBMC21010) were identified as TCRs reacting to HLA-A*02:01 restricted CMV pp65 antigen (NLVPMVATV). Top 1 clonotype in PBMC21002 was identified as TCRs reacting to HLA-A*02:01 restricted to influenza

A antigen (GILGFVFTL), and several TCRα or TCRβ were also identified as TCRα or TCRβ reacting to HLA-A*02:01 restricted to influenza A antigen (GILGFVFTL). Based on the frequency and TCR database findings, we selected clones having >10% of all clones and clones reacting CMV pp65 antigen in each case as a CMV-specific TCR candidate (Table 6). A total 10 clones (CMV TCR 1 ~ 10) were selected as CMV-specific TCR candidates.

Table 3. Single cell count of CMV activated T cells in PBMC21002, 21003 and 21010

Group	PBMC21002		PBMC21003		PBMC21010	
	count	percent (%)	count	percent (%)	count	percent (%)
$CD3E^{+}CD4^{+}CD8^{+}$	13	0.6	15	1.3	38	1.0
$CD3E^{+}CD4^{+}CD8^{-}$	0	0	0	0	5	0.1
$CD3E^{+}CD4^{-}CD8^{+}$	2,113	92.0	1,131	97.5	3739	97.2
$CD3E^{+}CD4^{-}CD8^{-}$	171	7.4	14	1.2	64	1.7
Total	**2,297**	**100**	**1,160**	**100**	**3,846**	**100**

Table 4. PBMC21002, PBMC21003 and PBMC21010 TCR clone of CMV-specific CD8+ T cells

Rank	PBMC21002 CMV-specific TCR information	Cells	Percent (%)
1	**TRAV24.TRAJ49.TRAC_TGTGCTAGGAACACCGGTAACCAGTTCTATTTT / TRBV6-5.TRBJ1-2.TRBD1.TRBC1_TGTGCCAGCAGTAAACAGACCGGGACAGGGAATTATGGCTACAC-CTTC**	**692**	**38.8**
2	**TRAV26-2.TRAJ43.TRAC_TGCATCCTTAACAATAACAATGACATGCGCTTT / TRBV30.TRBJ2-4.TRBC2_TGTGCCTGGAGTATCTCCGATCTAGCCAAAAACATTCAGTACTTC**	**315**	**17.6**
3	**TRAV24.TRAJ26.TRAC_TGTGCCCGTAACTATGGTCAGAATTTTGTCTTT / TRBV20-1.TRBJ2-7.TRBC2_TGCAGTGCTAGAGAAGTTGGTTCGCAGTCTTGGCACGAGCAGTACTTC**	**283**	**15.9**
4	**TRAV8-3.TRAJ37.TRAC_TGTGCTGGGCATGGCTCTAGCAACACAGGCAAACTAATCTTT / TRBV6-2.TRBJ1-1.TRBC1_TGTGCCAGCAGTTACCTACCCGGGACAGGTGAAGCTTTCTTT**	**106**	**5.9**
5	**TRAV24.TRAJ49.TRAC_TGTGCCCGTAACACCGGTAACCAGTTCTATTTT / TRBV6-5.TRBJ1-2.TRBC1_TGTGCCAGCAGTCCGCAAACAGGTACCGGGAACTATGGCTACACCTTC**	**49**	**2.7**

6	TRAV35.TRAJ50.TRAC_TGTGCTGGGCCGGAGAAAACCTCCTACGACAAGGTGATATTT / TRBV12-4.TRBJ1-2.TRBC1_TGTGCCAGCAGTTCGGCTAACTATGGCTACACCTTC	12	0.7
7	TRAV41.TRAJ48.TRAC_TGTGCTGTCAGATCTAACTTTGGAAATGAGAAATTAACCTTT / TRBV11-1.TRBJ2-6.TRBD1.TRBC2_TGTGCCAGCAGCTTCTGGGACAGGGCTTCTGGGGCCAAC-GTCCTGACTTTC	10	0.6
8	TRAV21.TRAJ40.TRAC_TGTGCTGTCCTCCCCCACGCTACCTCAGGAACCTACAAATACATCTTT / TRBV6-5.TRBJ1-1.TRBC1_TGTGCCAGCAGTTACTTGGGGACACAGAACACTGAAGCTTTCTTT	7	0.4
9	TRAV8-3.TRAJ37.TRAC_TGTGCTGGGGGGGGCTCTAGCAACACAGGCAAACTAATCTTT / TRBV6-5.TRBJ1-2.TRBC1_TGTGCCAGCAGTTACACGGCCGGGGGACAGAAATATGGCTACACCTTC	6	0.3
10	TRAV13-1.TRAJ52.TRAC_TGTGCAGCAATCAAGACCAGCGGTACTAGCTATGGAAAGCTGACATTT / TRBV6-5.TRBJ1-1.TRBC1_TGTGCCAGCAGTTATTTCGGGGGGAACACTGAAGCTTTCTTT	5	0.3

Rank	PBMC21003 CMV-specific TCR information	Cells	Percent (%)
1	TRAV24.TRAJ49.TRAC_TGTGCCTCGAACACCGGTAACCAGTTCTATTTT / TRBV6-5.TRBJ1-2.TRBD1.TRBC1_TGTGCCAGCAGTCCCCAAACCGGGACAGGGTTCTATGGCTACAC-CTTC	577	55.5
2	TRAV12-2.TRAJ42.TRAC_TGTGCCGTAGGAAGCCAAGGAAATCTCATCTTT / TRBV24-1.TRBJ2-7.TRBC2_TGTGCCACCAGTGACCCCCTGACGGCGTCCTACGAGCAGTACTTC	215	20.7
3	TRAV29/DV5.TRAJ50.TRAC_TGTGCAGCAAGCAATCCCCCCTCCTACGACAAGGTGATATTT / TRBV12-4.TRBJ1-2.TRBD1.TRBC1_TGTGCCAGCAGTGGGGCGGGGGGACTAAGCTATGGCTACACCTTC	97	9.3
4	TRAV35.TRAJ50.TRAC_TGTGCTGGGCCGACGAAAACCTCCTACGACAAGGTGATATTT / TRBV12-4.TRBJ1-2.TRBC1_TGTGCCAGCAGCTCAGCGTACTATGGCTACACCTTC	39	3.8
5	TRAV24.TRAJ49.TRAC_TGTGCCCGGAACACCGGTAACCAGTTCTATTTT / TRBV6-5.TRBJ1-2.TRBC1_TGTGCCAGCAGTCCGCAGACAGGGGCGACCTATGGCTACACCTTC	12	1.2
6	TRAV24.TRAJ49.TRAC_TGTGCCCGGAACACCGGTAACCAGTTCTATTTT / TRBV6-5.TRBJ1-2.TRBC1_TGTGCCAGCAGTCCGCAGACAGGGGCGACCTATGGCTACACCTTC; TRBV6-5.TRBJ1-2.TRBD1.TRBC1_TGTGCCAGCAGTCCCCAAACCGGGACAGGGTTCTATGGCTACAC-CTTC	7	0.7
7	TRAV8-1.TRAJ32.TRAC_TGTGCCGCTTCAACGGGTGGTGCTACAAACAAGCTCATCTTT / TRBV5-8.TRBJ2-7.TRBC2_TGTGCCAGCAGCCTATGGGCCGAGCAGTACTTC	6	0.6
8	TRAV17.TRAJ58.TRAC_TGTGCTACGGACTCTTATAAAGAAACCAGTGGCTCTAGGTTGACCTTT; TRAV12-3.TRAJ49.TRAC;TGTGCAACTTTTAACACCGGTAACCAGTTCTATTTT / TRBV12-4.TRBJ2-7.TRBC2_TGTGCCAGCAGTCCCGGGCTGCCCTACGAGCAGTACTTC	5	0.5
9	TRAV24.TRAJ49.TRAC_TGTGCCCGGAACACCGGTAACCAGTTCTATTTT / TRBV6-5.TRBJ1-2.TRBD1.TRBC1; TGTGCCAGCAGTCCCCAAACCGGGACAGGGTTCTATGGCTACAC-CTTC; TRBV6-5.TRBJ1-2.TRBC1_TGTGCCAGCAGTCCGCAGACAGGGGCGACCTATGGCTACACCTTC	5	0.5
10	TRAV8-3.TRAJ49.TRAC_TGTGCTGTGGCCTTTGGTAACCAGTTCTATTTT / TRBV27.TRBJ2-3.TRBC2_TGTGCCAGCAGTCTAGCGGGAGGGGCGGCAGATACGCAGTATTTT	5	0.5

Rank	PBMC21010 CMV-specific TCR information	Cells	Percent (%)

1	**TRAV24.TRAJ49.TRAC_TGTGCCCGGAACACCGGTAACCAGTTCTATTTT / TRBV6-5.TRBJ1-2.TRBC1_TGTGCCAGCAGTTACGCTACCGGGACAGCTTATGGCTACACCTTC**	**2121**	**58.8**
2	**TRAV3.TRAJ26.TRAC_TGTGCTGTATACTATGGTCAGAATTTTGTCTTT / TRBV28.TRBJ1-1.TRBC1_TGTGCCAGCAGTTTTCAGGGGTACACTGAAGCTTTCTTT**	**1099**	**30.4**
3	**TRAV29/DV5.TRAJ43.TRAC_TGTGCAGCAAGCGCGCAAGGTGACATGCGCTTT / TRBV6-5.TRBJ2-3.TRBC2;TRBV6-5.TRBJ1-2.TRBC1_TGTGCCAGCAGTACTGCAGATACGCAGTATTTT; TGTGCCAGCAGTTACGCTACCGGGACAGCTTATGGCTACACCTTC**	**135**	**3.7**
4	**TRAV29/DV5.TRAJ43.TRAC_TGTGCAGCAAGCGCGCAAGGTGACATGCGCTTT / TRBV6-5.TRBJ1-2.TRBC1;TRBV6-5.TRBJ2-3.TRBC2_TGTGCCAGCAGTTACGCTACCGG-GACAGCTTATGGCTAC ACCTTC;TGTGCCAGCAGTACTGCAGATACGCAGTATTTT**	**25**	**0.7**
5	**TRAV29/DV5.TRAJ43.TRAC_TGTGCAGCAAGCGCGCAAGGTGACATGCGCTTT / TRBV6-5.TRBJ2-3.TRBC2_TGTGCCAGCAGTACTGCAGATACGCAGTATTTT**	**15**	**0.4**
6	**TRAV39.TRAJ40.TRAC_TGTGCCGTGGCCCTTACCTCAGGAACCTACAAATACATCTTT / TRBV4-3.TRBJ2-3.TRBD1.TRBC2_TGCGCCAGCAGCCAAGATCTAAGAGGGACAGGGCGGACAGATAC-GCAGT ATTTT**	**10**	**0.3**
7	**TRAV19.TRAJ52.TRAC_TGTGCTCTGAGTGAGGGTGGTGGTACTAGCTATGGAAAGCTGACATTT / TRBV27.TRBJ2-1.TRBC2_TGTGCCAGCAAGAGATCCGGGACTAGCGGGTACAATGAGCAGTTCTTC**	**9**	**0.2**
8	**TRAV8-1.TRAJ34.TRAC_TGTGCCGTGTTAAATTATAACACCGACAAGCTCATCTTT / TRBV20-1.TRBJ1-4.TRBC1_TGCAGTGCTAGAGAAATGGGTGATGAAAAACTGTTTTTT**	**5**	**0.1**
9	**TRAV19.TRAJ49.TRAC_TGTGCTCTGAGTGAGTCACTAAACACCGGTAACCAGTTCTATTTT / TRBV7-6.TRBJ2-3.TRBC2_TGTGCCAGCAGCTTAGCGCCGGGGGTAGCGGGGATACTTGTTTTT**	**3**	**0.1**
10	**TRAV3.TRAJ26.TRAC;TRAV3.TRAJ35.TRAC_TGTGCTGTATACTATGGTCAGAATTTTGTCTTT; TGTGCTGTTTTCTTTGGGAATGTGCTGCATTGC / TRBV27.TRBJ2-2.TRBC2_TGTGCCAGCAGTTTATCGTCGGGGGTGCCCGGGGAGCTGTTTTTT**	**3**	**0.1**

Table 5. PBMC21002, PBMC21003 and PBMC21010 CMV specific TCR matching VDJ-DB and IEDB among top 10 clones

VDJ-DB	TCR	Antigen epitope	Antigen gene	Epitope species	HLA type
PBMC21002	TRA1	GILGFVFTL	M	Influenza A	A*02:01
		NLVPMVATV	pp65	CMV	A*02:01
	TRA2	NLVPMVATV	pp65	CMV	A*02
	TRA4	NLVPMVATV	pp65	CMV	A*02
	TRA5	GILGFVFTL	M	Influenza A	A*02:01
		NLVPMVATV	pp65	CMV	A*02:01
	TRA6	NLVPMVATV	pp65	CMV	A*02:01

	TRA8	AVFDRKSDAK	EBNA4	EBV	A*11:01
		TTDPSFLGRY	NSP3	SARS-CoV-2	A*01:01
		KLGGALQAK	IE1	CMV	A*03:01
		NLVPMVATV	pp65	CMV	A*02:01
	TRA9	GILGFVFTL	M	Influenza A	A*02:01
		RAKFKQLL	BZLF1	EBV	B*08:01
		NLVPMVATV	pp65	CMV	A*02:01
	TRB1	GILGFVFTL	M	Influenza A	A*02:01
	TRB2	NLVPMVATV	pp65	CMV	A*02:01
	TRB6	GILGFVFTL	M	Influenza A	A*02:01
		NLVPMVATV	pp65	CMV	A*02:01
	TRB10	NLVPMVATV	pp65	CMV	A*02:01
PBMC21003	TRA1	RLQSLQTYV	Spike	SARS-CoV-2	A*02
		SLLMWITQV	NY-ESO-1	HomoSapiens	A*02:01
		NLVPMVATV	pp65	CMV	A*02:01
	TRA2	GILGFVFTL	M	Influenza A	A*02:01
	TRA4	NLVPMVATV	pp65	CMV	A*02
	TRA5	GILGFVFTL	M	Influenza A	A*02:01
		NLVPMVATV	pp65	CMV	A*02:01
	TRA10	NLVPMVATV	pp65	CMV	A*02:01
	TRB4	NLVPMVATV	pp65	CMV	A*02:01
	TRB5	NLVPMVATV	pp65	CMV	A*02:01
	TRB8	NLVPMVATV	pp65	CMV	A*02:01
PBMC21010	TRA1	GILGFVFTL	M	Influenza A	A*02:01
		NLVPMVATV	pp65	CMV	A*02:01
	TRA2	NLVPMVATV	pp65	CMV	A*02:01
	TRA10	NLVPMVATV	pp65	CMV	A*02:01
	TRA2	NLVPMVATV	pp65	CMV	A*02:01
	TRA4	NLVPMVATV	pp65	CMV	A*02
IEDB	**TCR**	**Antigen epitope**	**Antigen gene**	**Epitope species**	**HLA type**
PBMC21002	TRB1	GILGFVFTL	M	Influenza A	A*02:01
	TRB2	NLVPMVATV	pp65	CMV	A*02:01
	TRB6	QELIRQGTDYKHW	N	SARS-CoV-2	HLA-B*44:02
		NLVPMVATV	pp65	CMV	A*02:01
PBMC21003	TRB4	NLVPMVATV	HCMVUL83	CMV	

	TRB8	NLVPMVATV, SEETGTLIV	HCMVUL83, envelope protein SARS-CoV2	CMV, SARS-CoV2	
	TRB10	TLIGDCATV	orf1ab polyprotein SARS-CoV2	SARS-CoV2	
PBMC21010	TRB2	NLVPMVATV, MGYINVFAFPFTIYSL	HCMVUL83, ORF10 protein SARS-CoV2	CMV, SARS-CoV2	
	TRB3	RQLLFVVEV	orf1ab polyprotein SARS-CoV2	SARS-CoV2	
	TRB1, TRB4	ELAGIGILTV	MART-1	HomoSapiens	

Table 6. Selected CMV-specific TCR candidates

PBMC	Clone rank	TRAV	TRAJ	TRAC	TRBV	TRBJ	TRBC	CMV TCR clone No.
21002	1	TRAV24	TRAJ49	TRAC	TRBV6-5	TRBJ1-2	TRBC1	CMV TCR1
21002	2	TRAV26-2	TRAJ43	TRAC	TRBV30	TRBJ2-4	TRBC2	CMV TCR2
21002	3	TRAV24	TRAJ26	TRAC	TRBV20-1	TRBJ2-7	TRBC2	CMV TCR3
21002	6	TRAV35	TRAJ50	TRAC	TRBV12-4	TRBJ1-2	TRBC1	CMV TCR4
21003	1	TRAV24	TRAJ49	TRAC	TRBV6-5	TRBJ1-2	TRBC1	CMV TCR5
21003	2	TRAV12-2	TRAJ42	TRAC	TRBV24-1	TRBJ2-7	TRBC2	CMV TCR6
21003	4	TRAV35	TRAJ50	TRAC	TRBV12-4	TRBJ1-2	TRBC1	CMV TCR7
21003	5	TRAV24	TRAJ49	TRAC	TRBV6-5	TRBJ1-2	TRBC1	CMV TCR8
21010	1	TRAV24	TRAJ49	TRAC	TRBV6-5	TRBJ1-2	TRBC1	CMV TCR9
21010	2	TRAV3	TRAJ26	TRAC	TRBV28	TRBJ1-1	TRBC1	CMV TCR10

2-2) EBV-specific TCR sequences

In EBV-specific T cells, there was the frequency of 89.3% (3,679/4,118), 93.1% (283/304), and 94.1% (5,020/5,332) of $CD3^+$ T cells per total cells and of which 64.9% (2,388/3,679), 64.7% (183/283), and 74.7% (3,748/5,020) were $CD3E^+CD4^-CD8^+$ cells in PBMC21002, 21003, and 21010, respectively (Table 7).

In the $CD3E^+CD4^-CD8^+$ group, dominant clones identified a high fraction as 60-80% of a group repertoire (Table 8). TCRα or TCRβ of top 10 clonotypes in each sample were also compared to the information of TCR database that includes TCR specific for the various antigens (Table 9). Several clonotypes (top 4 and top 9 in PBMC21002 and top 8 in PBMC21010) were identified as TCRs reacting to HLA-A*02:01 restricted to CMV pp65 antigen (NLVPMVATV). Top 2, top 4, and top 9 clonotypes in PBMC21002 were identified as TCRs reacting to HLA-A*02:01 restricted to influenza A antigen (GILGFVFTL), and several TCRα or TCRβ were also identified as TCRα or TCRβ reacting to HLA-A*02:01 restricted to influenza A antigen (GILGFVFTL). Because there were no confirmed EBV-reactive TCRs, we selected clones having >10% of all clones in each case as a EBV-specific TCR candidate (Table 10). A total 5 clones (EBV TCR 1 ~ 5) were selected as EBV-specific TCR candidates. Among the candidates, EBV TCR 2 was identical to CMV TCR 1 and EBV TCR 4 was identical to CMV TCR 5.

Table 7. In EBV specific T cell in PBMC21002, 21003 and 21010, Cell count according to presence/absence of CD3E, CD4 and CD8 gene expression

Group	PBMC21002		PBMC21003		PBMC21010	
	count	percent (%)	count	percent (%)	count	percent (%)
$CD3E^{+}CD4^{+}CD8^{+}$	5	0.1	26	9.2	43	0.9
$CD3E^{+}CD4^{+}CD8^{-}$	21	0.6	40	14.1	63	1.3
$CD3E^{+}CD4^{-}CD8^{+}$	2,388	64.9	183	64.7	3,748	74.7
$CD3E^{+}CD4^{-}CD8^{-}$	1,265	34.4	34	12.0	1,166	23.2
Total	**3,679**	**100**	**283**	**100**	**5,020**	**100**

Table 8. PBMC21002, PBMC21003 and PBMC21010 TCR clone of EBV-specific CD8+ T cells

Rank	PBMC21002 EBV-specific TCR information	Cells	Percent (%)
1	**TRAV8-4.TRAJ36.TRAC_TGTGCTGTGATGAGGCTTGAAACTGGGGCAAACAACCTCTTCTTT / TRBV28.TRBJ1-2.TRBC1_TGTGCCAGCAGCCTAACTTCAGGGAACTATGGCTACACCTTC**	609	35.1
2	**TRAV24.TRAJ49.TRAC_TGTGCTAGGAACACCGGTAACCAGTTCTATTTT / TRBV6-5.TRBJ1-2.TRBD1.TRBC1_TGTGCCAGCAGTAAACAGACCGGGACAGGGAATTATGGCTACACCTTC**	482	27.7
3	**TRAV24.TRAJ26.TRAC_TGTGCCCGTAACTATGGTCAGAATTTTGTCTTT / TRBV20-1.TRBJ2-7.TRBC2_TGCAGTGCTAGAGAAGTTGGTTCGCAGTCTTGGCACGAGCAGTACTTC**	88	5.1
4	**TRAV26-2.TRAJ43.TRAC_TGCATCCTTAACAATAACAATGACATGCGCTTT / TRBV30.TRBJ2-4.TRBC2_TGTGCCTGGAGTATCTCCGATCTAGCCAAAAACATTCAGTACTTC**	80	4.6
5	**TRAV10.TRAJ45.TRAC_TGTGTGGTGAGCTCGGAACCCTTCACAGGAGGAGGTGCTGACGGACTCACCTTT / TRBV30.TRBJ1-4.TRBC1_TGTGCCTGGAGTGTACGTCAGGGGCATGAAAAACTGTTTTTT**	48	2.8
6	**TRAV25.TRAJ32.TRAC_TGTGCAGGGACGAATTATGGTGGTGCTACAAACAAGCTCATCTTT / TRBV27.TRBJ2-1.TRBC2_TGTGCCAGCAGTCCCTTAATTTGGACAAACAATGAGCAGTTCTTC**	19	1.1
7	**TRAV12-2.TRAJ39.TRAC_TGTGCCGCAATAGCCTGGGATGCAGGCAACATGCTCACCTTT / TRBV30.TRBJ2-6.TRBC2_TGTGCCGGGTACTCTGGGGCCAACGTCCTGACTTTC**	14	0.8
8	**TRAV17.TRAJ11.TRAC_TGTGCTACGGAAGGGAATTCAGGATACAGCACCCTCACCTTT / TRBV6-5.TRBJ1-2.TRBC1_TGTGCCAGCAGTCAACAGGGGGGCAACTATGGCTACACCTTC**	11	0.6
9	**TRAV35.TRAJ50.TRAC_TGTGCTGGGCCGGAGAAAACCTCCTACGACAAGGTGATATTT / TRBV12-4.TRBJ1-2.TRBC1_TGTGCCAGCAGTTCGGCTAACTATGGCTACACCTTC**	11	0.6
10	**TRAV34.TRAJ39.TRAC_TGTGGAGCAGCCCTCAAAGGGGTAGGGGAAGATGCAGGCAACATGCTCACCTTT / TRBV2.TRBJ1-2.TRBD1.TRBC1_TGTGCCAGCAGTGAAATGGGGCAAATCTATGGCTACACCTTC**	10	0.6

Rank	PBMC21003 EBV-specific TCR information	Cells	Percent (%)
1	TRAV17.TRAJ11.TRAC_TGTGCTACGGTCGGGGGGTTCGGATACAGCACCCTCACCTTT / TRBV6-5.TRBJ1-2.TRBC1_TGTGCCAGCAGTTACCAGGGTGGTCAGTCTGATGGCTACACCTTC	60	38.7
2	TRAV24.TRAJ49.TRAC_TGTGCCTCGAACACCGGTAACCAGTTCTATTTT / TRBV6-5.TRBJ1-2.TRBD1.TRBC1_TGTGCCAGCAGTCCCCAAACCGGGACAGGGTTCTATGGCTACACCTTC	18	11.6
3	TRAV17.TRAJ11.TRAC_TGTGCTGCCGAAGGGAATTCAGGATACAGCACCCTCACCTTT / TRBV6-5.TRBJ1-2.TRBD1.TRBC1_TGTGCCAGCAGTGTACAGGGGGGCCGGGGTGGCTACACCTTC	15	9.7
4	TRAV29/DV5.TRAJ43.TRAC_TGTGCAGCAAGCGCGCAGAACAATGACATGCGCTTT / TRBV29-1.TRBJ1-2.TRBC1_TGCAGCGTTGCTGGGGCTGGCTATGGCTACACCTTC	12	7.7
5	TRAV6.TRAJ40.TRAC;TRAV17.TRAJ11.TRAC_TGTGCTCCCCTCTCAGGAACCTACAAATACATCTTT ;TGTGCTTCCGAGGGGAATTCAGGATACAGCACCCTCACCTTT / TRBV6-5.TRBJ1-2.TRBC1_TGTGCCAGCAGCTTACAGGGGGGTTCCAAGGGCTACACCTTC	7	4.5
6	TRAV17.TRAJ11.TRAC_TGTGCTTCCGAGGGGAATTCAGGATACAGCACCCTCACCTTT / TRBV6-5.TRBJ1-2.TRBC1_TGTGCCAGCAGCTTACAGGGGGGTTCCAAGGGCTACACCTTC	6	3.9
7	TRAV19.TRAJ27.TRAC_TGTGCTCTGAACACCAATGCAGGCAAATCAACCTTT / TRBV4-3.TRBJ2-1.TRBC2_TGCGCCAGCAGCCAAGATGGGACTAGCTACAATGAGCAGTTCTTC	4	2.6
8	TRAV17.TRAJ11.TRAC_TGTGCTACGGAGGGGAATTCAGGATACAGCACCCTCACCTTT / TRBV6-5.TRBJ1-2.TRBC1_TGTGCCAGCAGTTACCAAGGGGGAGTCAAGTATGGCTACACCTTC	3	1.9
9	TRAV12-2.TRAJ39.TRAC_TGTGCCGTGAACCGGGATAATGCAGGCAACATGCTCACCTTT / TRBV10-3.TRBJ2-7.TRBC2_TGTGCCATCACCAGGACAGACTCCTACGAGCAGTACTTC	2	1.3
10	TRAV13-1.TRAJ52.TRAC_TGTGCGGCTGCTGGTGGTACTAGCTATGGAAAGCTGACATTT / TRBV29-1.TRBJ2-1.TRBC2_TGCAGCGTTGAAGGGAGGTTTTACAATGAGCAGTTCTTC	2	1.3

Rank	PBMC21010 EBV-specific TCR information	Cells	Percent (%)
1	TRAV29/DV5.TRAJ43.TRAC_TGTGCAGCAAGCGCGCAAGGTGACATGCGCTTT_ TRBV6-5.TRBJ2-3.TRBC2_TGTGCCAGCAGTACTGCAGATACGCAGTATTTT	2,557	75.2
2	TRAV39.TRAJ40.TRAC_TGTGCCGTGGCCCTTACCTCAGGAACCTACAAATACATCTTT_ TRBV4-3.TRBJ2-3.TRBD1.TRBC2_TGCGCCAGCAGCCAAGATCTAAGAGGGACAGGGCGGACAGATACGCA GTATTTT	134	3.9
3	TRAV19.TRAJ52.TRAC_TGTGCTCTGAGTGAGGGTGGTGGTACTAGCTATGGAAAGCTGACATTT_ TRBV27.TRBJ2-1.TRBC2_TGTGCCAGCAAGAGATCCGGGACTAGCGGGTACAATGAGCAGTTCTTC	70	2.1
4	TRAV17.TRAJ11.TRAC_TGTGCTACGGAGGGCGATTCAGGATACAGCACCCTCACCTTT_ TRBV6-5.TRBJ1-2.TRBC1_TGTGCCAGCAGCCGACAGGGAGGGAGCTATGGCTACACCTTC	66	1.9
5	TRAV5.TRAJ10.TRAC_TGTGCAGAGCCGGGGATCACGGGAGGAGGAAACAAACTCACCTTT_ TRBV28.TRBJ1-2.TRBD1.TRBC1_TGTGCCAGCAGTTTATATATGGCAGGGGGCGGTGATGGCTACACCTTC	58	1.7
6	TRAV17.TRAJ11.TRAC_TGTGCTACGGAGGGCGATTCAGGATACAGCACCCTCACCTTT_	53	1.6

	TRBV6-5.TRBJ1-2.TRBC1;TRBV6-5.TRBJ2-3.TRBC2_TGTGCCAGCAGCCGACAGGGAGGGAGCTATGGCT ACACCTTC;TGTGCCAGCAGTACTGCAGATACGCAGTATTTT		
7	**TRAV24.TRAJ49.TRAC_TGTGCCCGGAACACCGGTAACCAGTTCTATTTT_ TRBV6-5.TRBJ2-3.TRBC2;TRBV6-5.TRBJ1-2.TRBC1_TGTGCCAGCAGTACTGCAGATACGCAGTATTTT; TGTGCCAGCAGTTACGCTACCGGGACAGCTTATGGCTACACCTTC**	38	1.1
8	**TRAV3.TRAJ26.TRAC_TGTGCTGTATACTATGGTCAGAATTTTGTCTTT_ TRBV28.TRBJ1-1.TRBC1_TGTGCCAGCAGTTTTCAGGGGTACACTGAAGCTTTCTTT**	31	0.9
9	**TRAV24.TRAJ49.TRAC_TGTGCCCGGAACACCGGTAACCAGTTCTATTTT_ TRBV6-5.TRBJ1-2.TRBC1_TGTGCCAGCAGTTACGCTACCGGGACAGCTTATGGCTACACCTTC**	30	0.9
10	**TRAV17.TRAJ11.TRAC_TGTGCTCCGGAGGGGAATTCAGGATACAGCACCCTCACCTTT_ TRBV6-5.TRBJ1-2.TRBC1_TGTGCCAGCAGTTACCAGGGAGGAAACTATGGCTACACCTTC**	29	0.9

Table 9. PBMC21002, PBMC21003 and PBMC21010 EBV specific TCR matching VDJ-DB and IEDB among top 10 clones

VDJ-DB	TCR	Antigen epitope	Antigen gene	Epitope species	HLA type
PBMC21002	TRA2	GILGFVFTL	M	InfluenzaA	A*02:01
		NLVPMVATV	pp65	CMV	A*02:01
	TRA4	NLVPMVATV	pp65	CMV	A*02
	TRA8	LLLGIGILV	BST2	HomoSapiens	A*02
		FLYALALLL	LMP2A	EBV	A*02:01
	TRA9	NLVPMVATV	pp65	CMV	A*02:01
	TRB2	GILGFVFTL	M	InfluenzaA	A*02:01
	TRB4	NLVPMVATV	pp65	CMV	A*02:01
	TRB9	GILGFVFTL	M	InfluenzaA	A*02:01
		NLVPMVATV	pp65	CMV	A*02:01
PBMC21003	TRA2	RLQSLQTYV	Spike	SARS-CoV-2	A*02
		SLLMWITQV	NY-ESO-1	HomoSapiens	A*02:01
		NLVPMVATV	pp65	CMV	A*02:01
	TRA7	KLGGALQAK	IE1	CMV	A*03:01
	TRA8	LLLGIGILV	BST2	HomoSapiens	A*02
		FLYALALLL	LMP2A	EBV	A*02:01
	TRA10	KLGGALQAK	IE1	CMV	A*03:01
PBMC21010	TRA4	GILGFVFTL	M	InfluenzaA	A*02:01

		FLYALALLL	LMP2A	EBV	A*02:01
		LLLGIGILV	BST2	HomoSapiens	A*02
		RAKFKQLL	BZLF1	EBV	B*08:01
	TRA7	GILGFVFTL	M	InfluenzaA	A*02:01
		NLVPMVATV	pp65	CMV	A*02:01
	TRA8	NLVPMVATV	pp65	CMV	A*02:01
	TRB8	NLVPMVATV	pp66	CMV	A*02:01
	TRB9	NLVPMVATV	pp67	CMV	A*02
	TRB10	FLYALALLL	LMP2A	EBV	A*02:01
IEDB	**TCR**	**Antigen epitope**	**Antigen gene**	**Epitope species**	**HLA type**
PBMC21002	TRB2	GILGFVFTL	Matrix protein 1	Influenza A	
	TRB4	NLVPMVATV	HCMVUL83	CMV	
	TRB9	QELIRQGTDYKHW	nucleocapsid phosphoprotein	SARS-CoV2	
		NLVPMVATV	HCMVUL83	CMV	
PBMC21010	TRB1	RQLLFVVEV	orf1ab polyprotein	SARS-CoV2	
	TRB8	MGYINVFAFPFTIYSL	ORF10 protein	SARS-CoV2	
		NLVPMVATV	HCMVUL83	CMV	
	TRB9	ELAGIGILTV	MART-1	HomoSapiens	
	TRB10	FLYALALLL	Latent membrane protein 2	EBV	

Table 10. Selected EBV-specific TCR candidates

PBMC	Clone rank	TRAV	TRAJ	TRAC	TRBV	TRBJ	TRBC	EBV TCR clone No.
21002	1	TRAV8-4	TRAV36	TRAC	TRBV28	TRBJ1-2	TRBC1	EBV TCR1
21002	2	TRAV24	TRAJ49	TRAC	TRBV6-5	TRBJ1-2	TRBC1	EBV TCR2
21003	1	TRAV17	TRAJ11	TRAC	TRBV6-5	TRBJ1-2	TRBC1	EBV TCR3
21003	2	TRAV24	TRAJ49	TRAC	TRBV6-5	TRBJ1-2	TRBC1	EBV TCR4
21010	1	TRAV29/DV5	TRAJ43	TRAC	TRBV6-5	TRBJ2-3	TRBC2	EBV TCR5

3) Transduction of specific TCRs to T cells and validation of TCR-T

3-1) CMV-specific TCR-T

Ten plasmids with CMV-specific TCR candidates were transduced into TCR knock-out (KO) Jurkat-NFAT-Luc cell line using lentiviral packing plasmid, and the expression level of CMV TCR was confirmed by FACS based on antibody of mouse TCRβ (mTCRβ) constant region on Day 1 and 7. On Day 1, CMV TCR 6 and CMV TCR 4 showed lower expression rates of 48.3% and 57.2%, respectively, but all 10 CMV-specific TCRs were expressed more than 90% on Day 7 (Fig. 4).

In the Jurkat (TCR KO)-NFAT-Luc cell line in which the expression of CMV-specific TCR candidates was confirmed, the level of luminescence expression (TCR activation by antigen) was checked 24 hours later using T2 cells pulsed with CMV peptide. Among the 10 CMV-specific TCR candidates, all candidates showed reactivity with CMV peptide. TCR 1, 5, 9 and 10 showed higher reactivity compared to other TCRs (Fig. 5).

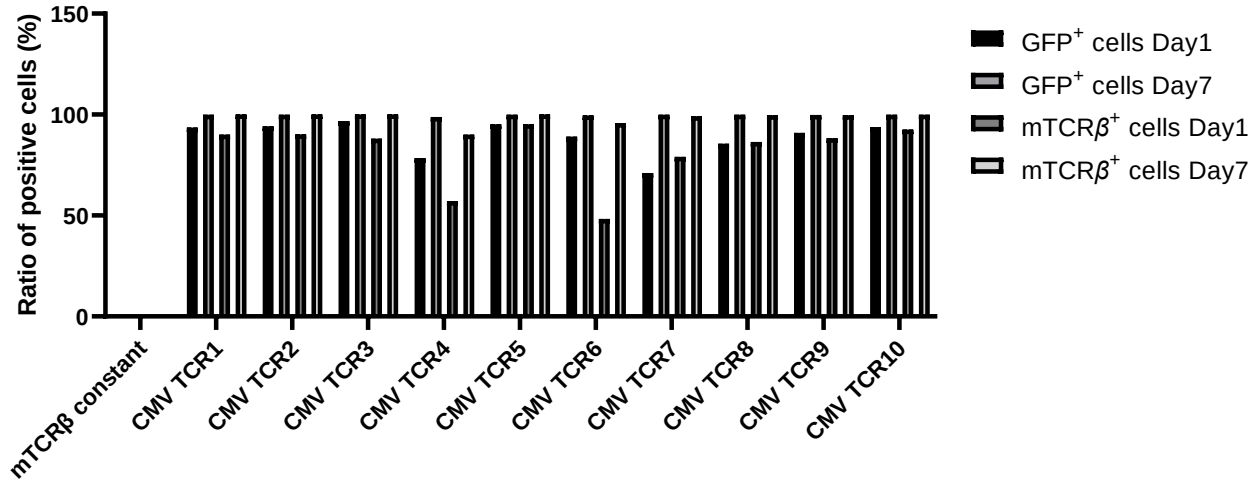

Fig. 4. Transduction efficiency of the selected CMV-specific TCR into the Jurkat (TCR KO)-NFAT-Luc cell line on Day 1 and 7.

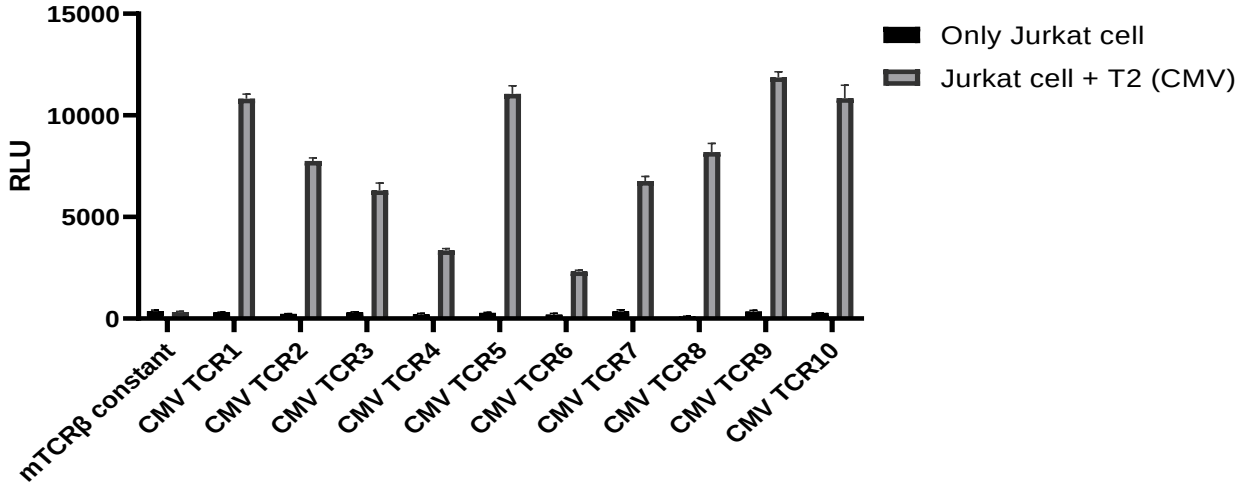

Fig. 5. Reaction between transduced Jurkat (TCR KO)-NFAT-Luc cell line and CMV peptide pulsed T2 on Day 7. The reactivity of the Jurkat (TCR KO)-NFAT-Luc cell line in which CMV-specific TCR was transduced by pulsing CMV peptide into the T2 cell line was confirmed by luciferase assay.

Next, 10 types of CMV-specific TCR candidates were transduced using lentiviral plasmid into healthy donor PBMCs, and expression was confirmed through mTCRβ expression on Day 7 and 14 (Fig. 6). Less than 5% of expression was identified on Day 14 in TCR 4 and 6, but TCR 10 showed more than 30% expression. Remaining TCR 1, 2, 3, 5, 7, and 9 showed about 10% of expression. IFN-γ secretion level was confirmed by ELISA assay by pulsing CMV peptide or influenza A into T2 cell line with transduced PBMCs. CMV-specific TCR 6 secreted the lowest IFN-γ (about 300 pg/ml), and about 650 pg/ml was secreted from TCR 10.

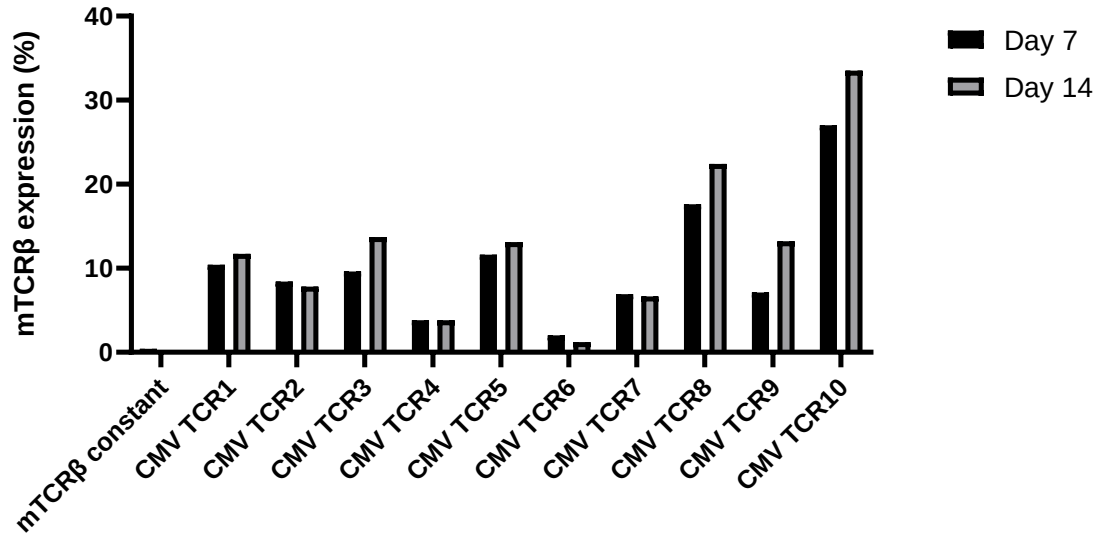

Fig. 6. Transduction efficiency of the selected CMV-specific TCR into healthy donor PBMCs on Day 7 and 14.

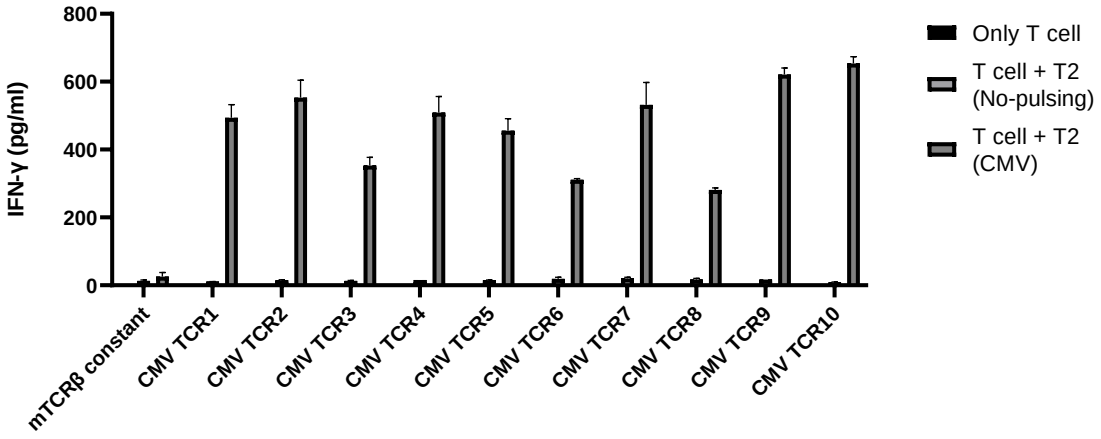

Fig. 7. Analysis of the reaction between CMV TCR-transduced PBMC and T2 cells pulsed with CMV peptide by IFN-γ ELISA.

3-2) EBV-specific TCR-T

Five EBV-specific TCR candidates were transduced in TCR KO Jurkat (TCR KO)-NFAT-Luc cell line through lentiviral plasmids. The expression level was measured by FACS using mTCRβ (Fig. 8). On Day 7, expression levels of all 5 types were over 90%.

Jurkat (TCR KO)-NFAT-Luc cells expressing EBV-specific TCR candidates were reacted with T2 cells pulsed with EBV peptides, and then luminescence was measured. Since the EBV-specific TCR candidates are likely to bind to CMV in the bioinformatics analysis, the CMV peptide was additionally pulsed to react. Only EBV TCR 3 specifically reacted with EBV peptides, and EBV TCR 2 and 4 had no response to EBV peptides but showed response to CMV peptide. Since EBV TCR 2 and 4 were identical to the clones of CMV TCR 1 and 5, respectively, it was observed that they responded to the CMV peptide (Fig. 9A). The EBV-6 peptide as a positive group, which differs from EBV peptide 3 in only one amino acid sequence and whose reactivity has already been confirmed in other papers, was also tested (Figure 9B, Supplement table 1). (20, 21) There was almost no difference in luminescence reactivity between EBV mix and EBV-6.

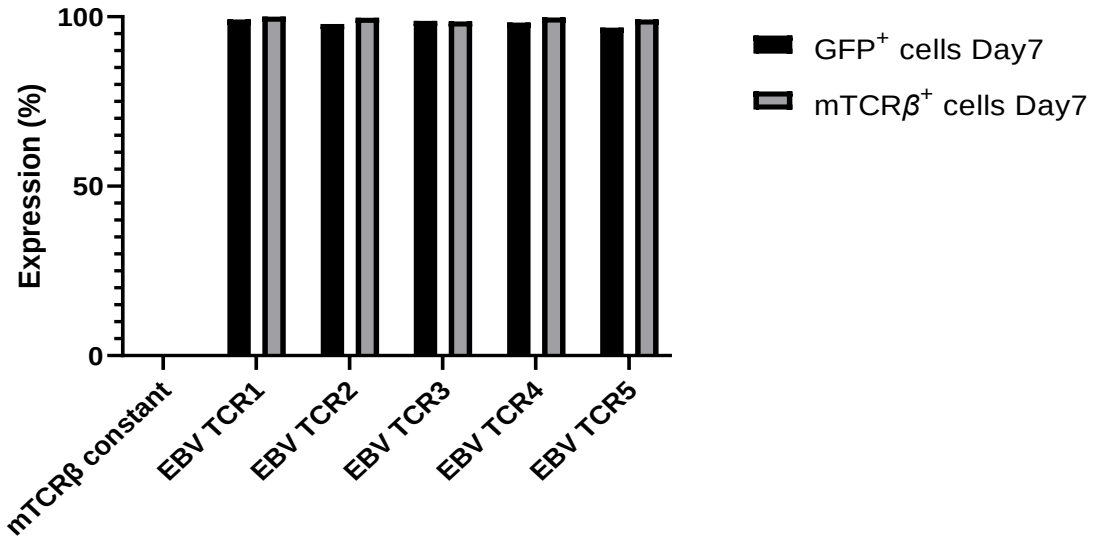

Fig. 8. Expression efficiency of EBV TCR expression in Jurkat (TCR KO)-NFAT-Luc cell line on Day 7.

A.

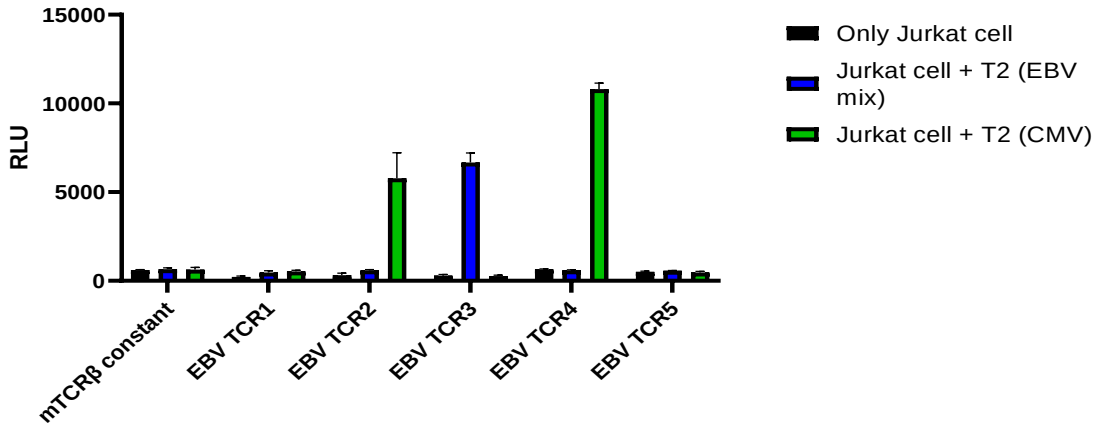

B.

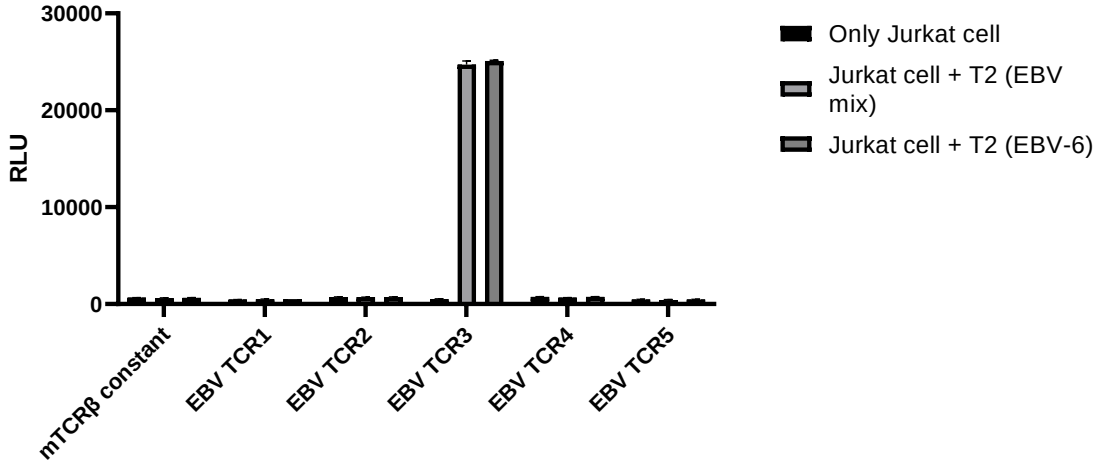

Fig. 9. The reactivity between the Jurkat (TCR KO)-NFAT-Luc cell line expressing EBV-specific TCR and T2 cells exposed to EBV or CMV peptides. A. Luminescence analysis between Jurkat (TCR KO)-NFAT-Luc cell line, which each expresses five EBV-specific TCRs, and T2 cells exposed to EBV mix or CMV peptides. B. Luminescence analysis between Jurkat (TCR KO)-NFAT-Luc cell line, each expressing five EBV-specific TCRs, and T2 cells exposed to EBV mix or EBV-6.

Since the reactivity was tested using all 5 types of EBV peptides that are expected to react, we checked the reactivity of the EBV TCR 3 with 5 types of EBV peptides to determine which peptides were reacted. Of the five EBV peptides, only EBV peptide 3 (FLYALALLI) was confirmed to react with EBV TCR 3, and little reaction with other peptides (LTAGFLIFL, CLGGLLTMC, TYGPVFMCL, RYCCYYCLTL) was identified (Fig. 10).

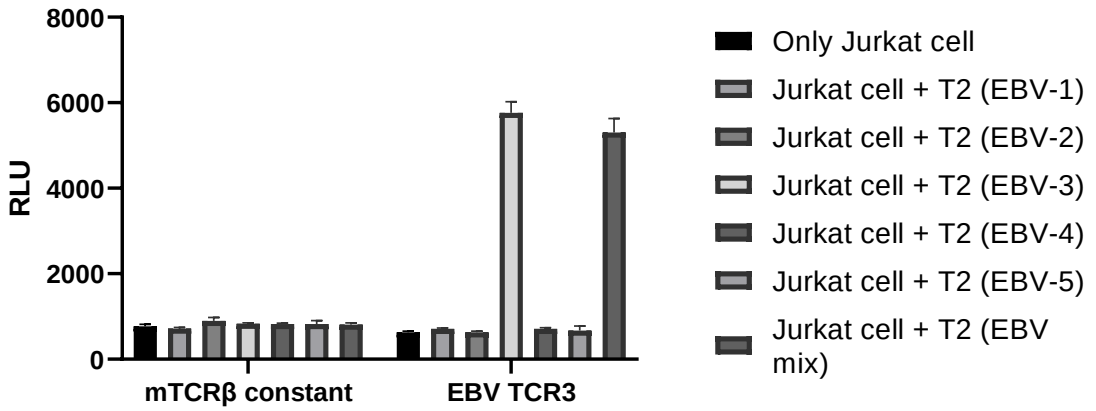

Fig. 10. Investigation of reactions of Jurkat (TCR KO)-NFAT-Luc cells expressing each EBV peptide and EBV TCR 3.

To confirm whether EBV-specific TCR candidates are applicable to PBMCs, we transduced all five candidates into healthy PBMCs and tested their reactivity. The expression level of EBV TCR in $CD3^+$ T cells on Day 14 was the lowest in EBV TCR 5 at 8.8%, the highest in EBV TCR 1 at 43.1%, and 25.1%, 15.9% and 15.9% in EBV TCR 2, 3 and 4, respectively (Fig. 11). As a result of the level of IFN-γ by co-culture with T2 cells pulsing EBV peptide, only EBV peptide 3 reacted with EBV TCR 3. In addition, EBV peptide 6 (FLYALALLL), which is one amino acid changed in EBV peptide 3, was also pulsed to confirm the reactivity, and the response was not significantly different from that of EBV peptide 3 (Fig. 12).

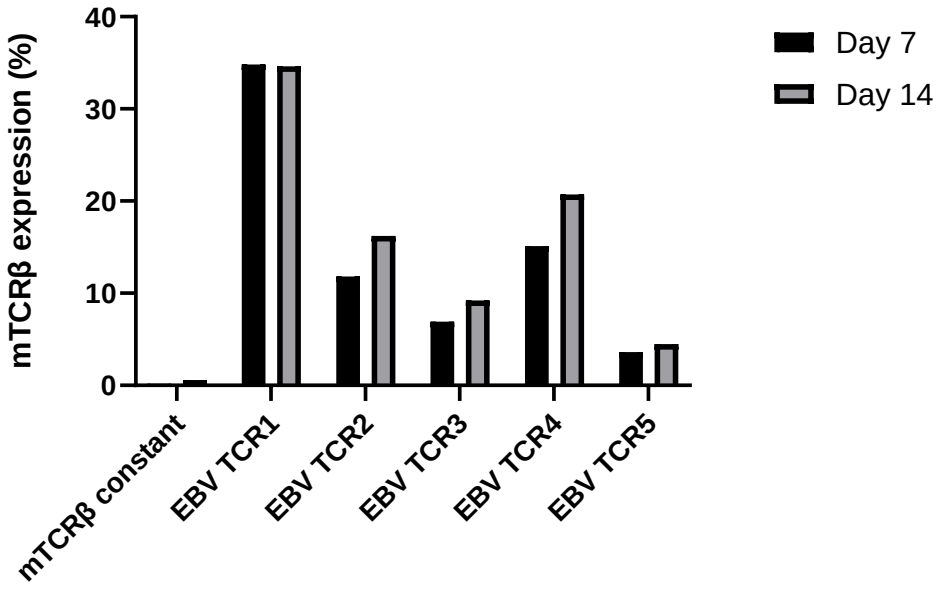

Fig. 11. Transduction efficiency of EBV-specific TCR into healthy donor PBMCs. The expression of mTCRβ was analyzed using flow cytometry on Day 7 and 14.

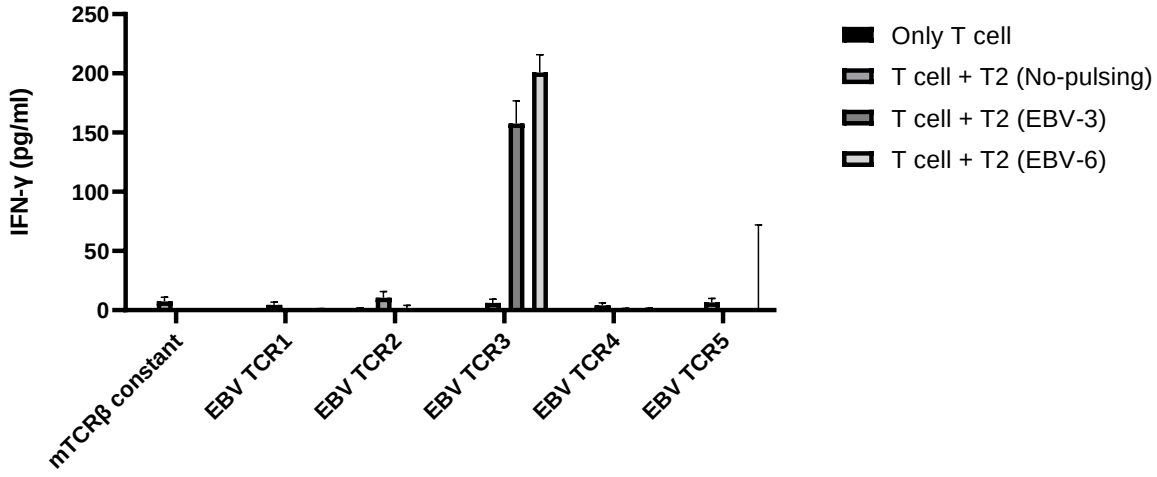

Fig. 12. Analysis of the reaction between EBV TCR-transduced PBMCs and T2 cells pulsed with EBV peptides.

Discussion

Recently, the importance of immunotherapy using TCR in neoantigen-specific T cells has been emerged in cancer treatment..(15, 22-24) Various methods for isolating antigen-specific T cells using molecules such as 4-1BB and PD-1 are investigated.(25-28) In addition to identifying neoantigens, isolating antigen-specific T cells using previously known tumor-derived antigens such as EBV and CMV has been studied.(29, 30)

Tetramers have been widely used for isolating T cells, but they have limitation that specific tetramers should be designed for each experiment and they cost high to make each specific antigen and MHC type.(16, 31, 32) Hong et al. compared three molecules (CD137, IFN- γ, and tetramer) to isolate $CD8^+$ T cells which are activated by CMV, and analyzed the TCR repertoires.(33) They suggested that separation using CD137 exhibited the highest sensitivity.(33) However, another study proposed that TCR analysis using CFSE is more sensitive and can secure more clonotypes than using CD137.(34) Usually, antigen presenting cells and $CD8^+$ T cells exposed to neoantigen are co-cultured to analyze neoantigen specific TCR.(24) Dextramer has been used to separate $CD8^+$ T cells that react to neoantigen, and takes about 2 weeks to separate (24) In this study, we illustrated a novel method using CFSE to isolate antigen-specific $CD8^+$ T cells which takes about a week, showing more cost and time-effectiveness than previously reported methods.

Isolated CD8+ cells from heathy donor PBMC showed most responsive to CMV at day 9. Co-culture with IL-2 was performed from day 2 because IL-2 induces non-specific proliferation when co-cultured from the start. Considering that the half-life of IL-2 is 15-30 minutes, the design was divided into groups on days 4 and 7 or without IL-2.(35) To identify the difference according to the culture environment, we used 96-well plate and

15ml PP tube. In both 96-well plate and PP tube, the proliferation of G1 without IL-2 was significantly lower than that of other groups. In addition, proliferation was increased in both the G2 and G3 conditions with replacing IL-2 containing media 1 or 2 times on Day 2 and 7, and G4 conditions with replacing IL-2 containing media on Day 2, Day 4, and Day 7. In negative control group, which treated with DMSO, proliferation occurs on Day 9, so we decided to isolate the cells on Day 7. At Day-7, proliferation level was higher in the G2 and G3 conditions than in the G4 condition. Same results of PBMC21002 were observed in the case of PBMC21010 when performed in PP tube. Therefore, we suggested as effective method for isolating $CD8^{+}CFSE^{-}$ cells and $CD8^{-}CFSE^{-}$ cells on Day 7 under G2 conditions using healthy donor PBMC.

Sorted cells produced a VDJ library through 10X GENOMICS, and the most frequently noted 10 clones were searched in the TCR database including VDJDB and IEDB. Clones with more than 10% frequency and previously identified known TCRs for CMV antigen were selected for antigen specific TCR candidates.

In order to validate CMV and EBV-specific TCR candidates, transduced Jurkat (TCR KO)-NFAT-Luc cells and PBMCs were evaluated for reactivity through the antigen presenting T2 cells which is stimulated by CMV or EBV peptide. Reaction was confirmed in all 10 types of CMV-specific TCR candidates and in EBV TCR 3. It is considered that TCR can be sufficiently confirmed in cell line, because the patterns of reactivity in cell line and PBMC were similar.

We performed TCR sequence analysis using CMV or EBV antigens, which have already been studied extensively, but recently, Okada et al. used PBMC donated from a healthy donor with the HLA:A*24:02 phenotype to develop TCR-T for multiple myeloma

mutants.(36) The TCR repertoire was analyzed through single cell TCR sequencing that reacts with neoantigen.(36) The analyzed TCR actually confirmed its reaction with neoantigen in vitro, and tumor regression was observed in in vivo experiments, clearly showing its potential as TCR-T therapy for multiple myeloma.(36)

A search of the TCR database revealed possible reactions to influenza A, CMV, or EBV. As a result of analyzing the clones for the selected EBV-specific TCR, two of the five clones were found to be TCRs that reacted to CMV peptides, and it was confirmed that they were reactive in vitro as well. Because the analyzed TCR has a CDR3 region with only a few amino sequence differences in the V and J segments that react with CMV(37, 38), EBV(37, 38), and influenza A(39), reactive clones may overlap. It is said that this difference in TCR repertoire is largely influenced by TCR β-chains.(40, 41) Therefore, the possibility of using TCR β-chains as a marker to analyze CMV-specific TCR was also raised.(42) TCR repertoire according to TCR β-chains continues to be studied in recent years, and analysis of TCR β-chains according to antigen also requires further research in the future.

Neoantigen-specific T cell receptor-engineered T cells using adoptive cell therapy can be attractive therapeutic targets for treatment of unresectable cancers. Our method provides relatively time and cost-effective way to identify neoantigen specific TCRs. Further studies for validation of our protocol with fresh tumors are needed.

In conclusion, we established an optimal proliferative condition to isolate antigen-specific T cells from healthy donor PBMCs. In addition, we isolated proliferating $CD8^+$ T cells reacting with CMV and EBV peptides. TCR sequence analysis also exhibited a reaction with CMV and EBV peptides in vitro. This methodology can be a cost and time

effective way to identify neoantigen specific T cells and TCRs which can be novel potential targets for immunotherapy.

Reference

1. Das S, Johnson DB. Immune-related adverse events and anti-tumor efficacy of immune checkpoint inhibitors. Journal for immunotherapy of cancer. 2019;7(1):1-11.
2. Tang H, Liang Y, Anders RA, Taube JM, Qiu X, Mulgaonkar A, et al. PD-L1 on host cells is essential for PD-L1 blockade–mediated tumor regression. The Journal of clinical investigation. 2018;128(2):580-8.
3. Rotte A. Combination of CTLA-4 and PD-1 blockers for treatment of cancer. Journal of Experimental & Clinical Cancer Research. 2019;38:1-12.
4. Jenkins RW, Barbie DA, Flaherty KT. Mechanisms of resistance to immune checkpoint inhibitors. British journal of cancer. 2018;118(1):9-16.
5. Van der Leun AM, Thommen DS, Schumacher TN. CD8+ T cell states in human cancer: insights from single-cell analysis. Nature Reviews Cancer. 2020;20(4):218-32.
6. Poorebrahim M, Mohammadkhani N, Mahmoudi R, Gholizadeh M, Fakhr E, Cid-Arregui A. TCR-like CARs and TCR-CARs targeting neoepitopes: An emerging potential. Cancer gene therapy. 2021;28(6):581-9.
7. Springuel L, Lonez C, Alexandre B, Van Cutsem E, Machiels J-PH, Van Den Eynde M, et al. Chimeric antigen receptor-T cells for targeting solid tumors: current challenges and existing strategies. BioDrugs. 2019;33:515-37.
8. Freeman JD, Warren RL, Webb JR, Nelson BH, Holt RA. Profiling the T-cell receptor beta-chain repertoire by massively parallel sequencing. Genome research. 2009;19(10):1817-24.
9. Robins HS, Campregher PV, Srivastava SK, Wacher A, Turtle CJ, Kahsai O, et al. Comprehensive assessment of T-cell receptor β-chain diversity in αβ T cells. Blood, The Journal of the American Society of Hematology. 2009;114(19):4099-107.
10. Hou X, Wang L, Ding Y, Xie Q, Diao H. Current status and recent advances of next generation sequencing techniques in immunological repertoire. Genes & Immunity. 2016;17(3):153-64.
11. Pai JA, Satpathy AT. High-throughput and single-cell T cell receptor sequencing technologies. Nature methods. 2021;18(8):881-92.
12. Lay L, Stroup B, Payton JE. Validation and interpretation of IGH and TCR clonality

testing by Ion Torrent S5 NGS for diagnosis and disease monitoring in B and T cell cancers. Practical Laboratory Medicine. 2020;22:e00191.

13. Guo X, Zhang Y, Zheng L, Zheng C, Song J, Zhang Q, et al. Global characterization of T cells in non-small-cell lung cancer by single-cell sequencing. Nature medicine. 2018;24(7):978-85.

14. Pan R-Y, Chung W-H, Chu M-T, Chen S-J, Chen H-C, Zheng L, et al. Recent development and clinical application of cancer vaccine: targeting neoantigens. Journal of immunology research. 2018;2018.

15. Xie N, Shen G, Gao W, Huang Z, Huang C, Fu L. Neoantigens: promising targets for cancer therapy. Signal Transduction and Targeted Therapy. 2023;8(1):9.

16. Hunsucker SA, McGary CS, Vincent BG, Enyenihi AA, Waugh JP, McKinnon KP, et al. Peptide/MHC Tetramer–Based Sorting of CD8+ T Cells to a Leukemia Antigen Yields Clonotypes Drawn Nonspecifically from an Underlying Restricted Repertoire. Cancer immunology research. 2015;3(3):228-35.

17. Watanabe K, Suzuki S, Kamei M, Toji S, Kawase T, Takahashi T, et al. CD137-guided isolation and expansion of antigen-specific CD8 cells for potential use in adoptive immunotherapy. International journal of hematology. 2008;88:311-20.

18. Parkhurst M, Gros A, Pasetto A, Prickett T, Crystal JS, Robbins P, et al. Isolation of T-cell receptors specifically reactive with mutated tumor-associated antigens from tumor-infiltrating lymphocytes based on CD137 expression. Clinical cancer research. 2017;23(10):2491-505.

19. Pasetto A, Gros A, Robbins PF, Deniger DC, Prickett TD, Matus-Nicodemos R, et al. Tumor-and neoantigen-reactive T-cell receptors can be identified based on their frequency in fresh tumor. Cancer immunology research. 2016;4(9):734-43.

20. Straathof KC, Leen AM, Buza EL, Taylor G, Huls MH, Heslop HE, et al. Characterization of latent membrane protein 2 specificity in CTL lines from patients with EBV-positive nasopharyngeal carcinoma and lymphoma. The Journal of Immunology. 2005;175(6):4137-47.

21. Su S, Zou Z, Chen F, Ding N, Du J, Shao J, et al. CRISPR-Cas9-mediated disruption of PD-1 on human T cells for adoptive cellular therapies of EBV positive gastric cancer. Oncoimmunology. 2017;6(1):e1249558.

22. Morgan RA, Chinnasamy N, Abate-Daga D, Gros A, Robbins PF, Zheng Z, et al. Cancer regression and neurological toxicity following anti-MAGE-A3 TCR gene therapy. Journal of immunotherapy. 2013;36(2):133-51.

23. Matsuda T, Leisegang M, Park J-H, Ren L, Kato T, Ikeda Y, et al. Induction of neoantigen-specific cytotoxic T cells and construction of T-cell receptor–engineered T cells for ovarian cancer. Clinical Cancer Research. 2018;24(21):5357-67.

24. Kato T, Matsuda T, Ikeda Y, Park J-H, Leisegang M, Yoshimura S, et al. Effective screening of T cells recognizing neoantigens and construction of T-cell receptor-engineered T cells. Oncotarget. 2018;9(13):11009.

25. Seliktar-Ofir S, Merhavi-Shoham E, Itzhaki O, Yunger S, Markel G, Schachter J, et al. Selection of shared and neoantigen-reactive T cells for adoptive cell therapy based on CD137 separation. Frontiers in immunology. 2017;8:1211.

26. Parkhurst M, Robbins P, Rosenberg S. Isolation of T cell receptors specifically reactive with mutated tumor associated antigens. Journal for immunotherapy of cancer. 2014;2:1-2.

27. Yossef R, Tran E, Deniger DC, Gros A, Pasetto A, Parkhurst MR, et al. Enhanced detection of neoantigen-reactive T cells targeting unique and shared oncogenes for personalized cancer immunotherapy. JCI insight. 2018;3(19).

28. Gros A, Tran E, Parkhurst MR, Ilyas S, Pasetto A, Groh EM, et al. Recognition of human gastrointestinal cancer neoantigens by circulating PD-1+ lymphocytes. The Journal of clinical investigation. 2019;129(11):4992-5004.

29. Kamga L. Conserved Features of the T Cell Receptor Repertoire Contribute to the Persistence of EBV-Specific CD8 T Cells. 2019.

30. Jiang W, Clancy LE, Avdic S, Sutrave G, Street J, Simms R, et al. Third-party CMV- and EBV-specific T-cells for first viral reactivation after allogeneic stem cell transplant. Blood Advances. 2022;6(17):4949-66.

31. Cohen CJ, Gartner JJ, Horovitz-Fried M, Shamalov K, Trebska-McGowan K, Bliskovsky VV, et al. Isolation of neoantigen-specific T cells from tumor and peripheral lymphocytes. The Journal of clinical investigation. 2015;125(10):3981-91.

32. Abdelaal HM, Cartwright EK, Skinner PJ. Detection of antigen-specific T cells using in situ MHC tetramer staining. International journal of molecular sciences.

2019;20(20):5165.
33. Hong C-H, Pyo H-S, Baek I-C, Kim T-G. Rapid identification of CMV-specific TCRs via reverse TCR cloning system based on bulk TCR repertoire data. Frontiers in Immunology. 2022;13:1021067.
34. Klinger M, Kong K, Moorhead M, Weng L, Zheng J, Faham M. Combining next-generation sequencing and immune assays: a novel method for identification of antigen-specific T cells. PLoS One. 2013;8(9):e74231.
35. Malek TR, Castro I. Interleukin-2 receptor signaling: at the interface between tolerance and immunity. Immunity. 2010;33(2):153-65.
36. Okada M, Shimizu K, Nakazato H, Yamasaki S, Fujii S-i. Detection of mutant antigen-specific T cell receptors against multiple myeloma for T cell engineering. Molecular Therapy-Methods & Clinical Development. 2023;29:541-55.
37. Miconnet I, Marrau A, Farina A, Taffé P, Vigano S, Harari A, et al. Large TCR diversity of virus-specific CD8 T cells provides the mechanistic basis for massive TCR renewal after antigen exposure. The Journal of Immunology. 2011;186(12):7039-49.
38. Venturi V, Chin HY, Asher TE, Ladell K, Scheinberg P, Bornstein E, et al. TCR β-chain sharing in human CD8+ T cell responses to cytomegalovirus and EBV. The Journal of Immunology. 2008;181(11):7853-62.
39. Chen G, Yang X, Ko A, Sun X, Gao M, Zhang Y, et al. Sequence and structural analyses reveal distinct and highly diverse human CD8+ TCR repertoires to immunodominant viral antigens. Cell reports. 2017;19(3):569-83.
40. Deschler K, Rademacher J, Lacher SM, Huth A, Utzt M, Krebs S, et al. Antigen-specific immune reactions by expanded CD8+ T cell clones from HLA-B* 27-positive patients with spondyloarthritis. Journal of Autoimmunity. 2022;133:102901.
41. Hou X, Zeng P, Zhang X, Chen J, Liang Y, Yang J, et al. Shorter TCR β-chains are highly enriched during thymic selection and antigen-driven selection. Frontiers in Immunology. 2019;10:299.
42. Huth A, Liang X, Krebs S, Blum H, Moosmann A. Antigen-specific TCR signatures of cytomegalovirus infection. The Journal of Immunology. 2019;202(3):979-90.

국문요약

항원 특이적 T 세포를 이용한 입양세포치료는 암 환자에게 유망한 치료 방법입니다. 따라서 입양세포치료를 위한 효과적인 표적을 찾기 위해서 항원 특이적 T 세포를 분리하고 해당 T 세포 수용체 (TCR)를 확인하는 새로운 방법이 필요합니다. 우리는 CFSE로 염색된 PBMC를 항원 펩타이드로 자극하여 증식이 일어나는 항원 특이적 T 세포를 분리하여 평가했다. 또한, 우리는 CMV 및 EBV 특이적인 TCR 서열을 분석하고, 항원 특이적 TCR은 T 세포로 형질도입 함으로써 TCR-T의 유효성을 평가했습니다. 건강한 기증자 PBMC로부터 분리된 $CD8^+$ 세포는 최소한의 IL-2를 사용하는 G2 조건으로 7일째에 CMV 및 EBV에 반응하여 가장 많은 증식이 나타났습니다. 또한 TCR 서열 분석은 in vitro에서 CMV 및 EBV 펩타이드에 대한 반응성을 확인했습니다. 반응성은 10가지 모두의 CMV 특이적 TCR과 EBV TCR 3에서 확인되었습니다. 결론적으로, 신생항원 특이적 T 세포와 TCR을 확인하는 방법은 비용 및 시간적으로 효율적인 방법이 될 수 있으며, 이는 면역치료의 새로운 잠재적인 표적이 될 수 있습니다.